

Studying chirality imbalance with quantum algorithms

Alexander M. Czajka,^{1,2,*} Zhong-Bo Kang,^{1,2,3,4,†} Yuxuan Tee,^{1,‡} and Fanyi Zhao^{1,2,3,§}

¹*Department of Physics and Astronomy, University of California, Los Angeles, CA 90095, USA*

²*Mani L. Bhaumik Institute for Theoretical Physics,
University of California, Los Angeles, CA 90095, USA*

³*Center for Quantum Science and Engineering, University of California, Los Angeles, CA 90095, USA*

⁴*Center for Frontiers in Nuclear Science, Stony Brook University, Stony Brook, NY 11794, USA*

To describe the chiral magnetic effect, the chiral chemical potential μ_5 is introduced to imitate the impact of topological charge changing transitions in the quark-gluon plasma under the influence of an external magnetic field. We employ the (1+1) dimensional Nambu-Jona-Lasinio (NJL) model to study the chiral phase structure and chirality charge density of strongly interacting matter with finite chiral chemical potential μ_5 in a quantum simulator. By performing the Quantum imaginary time evolution (QITE) algorithm, we simulate the (1+1) dimensional NJL model on the lattice at various temperature T and chemical potentials μ, μ_5 and find that the quantum simulations are in good agreement with analytical calculations as well as exact diagonalization of the lattice Hamiltonian.

I. INTRODUCTION

In quantum chromodynamics (QCD), several major challenges have gained considerable attention, including how the vacuum structures of QCD are affected in extreme environments [1]. QCD research in hot and dense conditions is of great importance, not only from a purely theoretical perspective, but also for its numerous applications to the studies of the quark matter in the ultradense compact stars [2–8], and the Quark-Gluon Plasma (QGP) which is abundantly produced in relativistic collisions of heavy ions [9, 10]. Studying how non-perturbative features of QCD are affected by thermal excitations at high temperatures T and by baryon-rich matter at finite chemical potentials μ [11] is highly interesting.

Besides the effects of finite T and μ , the influence of a strong magnetic field B is an exciting topic relevant to phenomenology in relativistic heavy-ion collisions, where strong magnetic fields are generated in non-central collisions [12–17]. Many studies have been conducted on the effect of magnetic fields on the QCD vacuum [18–24], and it has been determined that magnetic fields B act as a catalyst of dynamical chiral symmetry breaking [25–27]. In the presence of a magnetic field, a finite current is induced along the direction of the field lines due to the anomalous production of an imbalance between right- and left-handed quarks, namely that the number of right-handed quarks N_R ¹ is not equal to the number of left-handed quarks N_L . This effect is known as the Chiral Magnetic Effect (CME) [28–30].

The axial anomaly and topological objects in QCD are

the fundamental physics of the CME. At low or zero temperatures, the change of non-trivial topological structure is related to instanton [31, 32] with the quantum tunneling effect. However, at finite temperatures, the transition is caused by sphalerons [33–35] and the chiral asymmetry shows up. Unbalanced left- and right-handed quarks can produce observable effects that can be used to investigate topological \mathcal{P} - and \mathcal{CP} -odd excitations [36–42]. Thus the CME is a phenomenologically and experimentally interesting effect of the strong magnetic field in heavy-ion collisions. In [43], an observable sensitive to local \mathcal{P} - and \mathcal{CP} -violation has been proposed for experiments. Measurements of charge correlations were made by STAR at RHIC [14, 44–48], where conclusive evidence of charge azimuthal correlations was observed, which could be a possible result from CME with local \mathcal{P} - and \mathcal{CP} -odd effects. Furthermore, consistent experimental data was provided by ALICE [49–53] and CMS [54, 55] at the LHC, where the azimuthal correlator was measured to search for the CME in heavy-ion collisions.

By introducing a finite chiral chemical potential μ_5 that imitates the effects of the topological charge changing transitions, one can study the QCD phase diagram [56] as well as the thermal behavior of the total chirality charge $N_5 = N_R - N_L$ under the influence of an external magnetic field at finite temperature T and baryon chemical potential μ . At sufficiently high temperatures/densities, the strongly-interacting matter goes through a deconfinement phase transition from hadronic matter to quark-gluon plasma, and it is possible that a chirality charge is produced in the phase transition as a result of the flip of fermion helicity in the interaction with the gauge field. Moreover, it has been demonstrated that immediately after a heavy-ion collision, the chirality charge comes to and stays at an equilibrium value [7, 57, 58]. In light of these considerations, it is evident that exploring the chiral imbalance in the QCD phase diagrams is crucial for the description of heavy-ion collisions.

To study the chiral magnetic effect and the QCD chiral

* aczajka74@physics.ucla.edu

† zkang@ucla.edu

‡ yxtee0824@gmail.com

§ fanyizhao@physics.ucla.edu

¹ More precisely, N_R the number of right-handed quarks minus the number of left-handed antiquarks, with N_L defined analogously.

phase transition, the Nambu-Jona-Lasinio (NJL) model [59, 60] has been playing an important role for many years [5, 61–70]. As an effective model for QCD, the NJL model is amenable to analytical calculations at finite temperature T and chemical potentials μ and μ_5 .

In recent years, lattice QCD simulations have significantly improved our understanding of the QCD phase diagram at zero or small chemical potentials μ [71–76]. However, as a result of the sign problem [77], at finite μ , Monte-Carlo simulation is unable to be directly applied because the fermion determinant becomes complex, and its phase fluctuations prohibit its interpretation as a probability density [71]. As a result, the sign problem is a fundamental impediment to comprehending the phase structure of nuclear matter. This is, however, not a flaw in QCD theory, but rather in the attempt to mimic quantum statistics via the functional integral using a classical Monte Carlo approach.

Fortunately, as indicated in [56, 78], the statistical properties of a quantum computer can be used to obviate the necessity for a Monte Carlo study by modeling the lattice system on a quantum computer. And there have been abundant developments in applying quantum computing to solving physics problems. In recent years, it has been shown that using the current generation of Noisy Intermediate-Scale Quantum (NISQ) technology that quantum computers can solve complex problems like simulating thermal properties [79–89], evaluating ground states and real-time dynamics [78, 90–104], modeling many-body systems and relativistic effects [105–145], etc. Though digital quantum simulations on thermal physical systems were researched earlier on, finite-temperature physics is less well-known and still has to be improved on quantum computers [146]. Several algorithms for imaginary time evolution on quantum computers, both with and without ansatz dependency, have been introduced in recent years. In particular, the Quantum Imaginary Time Evolution (QITE) algorithm applies a unitary operation to simulate imaginary time evolution and has been performed to simulate energy and magnetism in the Transverse Field Ising Model (TFIM) [147], the chiral condensate in NJL model [148] and so on. This study, along with previous studies, demonstrates that NISQ quantum computers can provide consistent and correct answers to physical problems that cannot be solved efficiently or effectively using classical computing algorithms, indicating promising future applications of quantum computing in non-perturbative QCD and beyond.

The remainder of this paper is organized as follows: In Sec. II, we provide a brief description of the $(1+1)$ -dimensional NJL model and the QITE algorithm used for the quantum simulation. In Sec. III, we show the analytic calculations of chiral condensate and chirality charge density at finite temperature, baryon and chiral chemical potentials. We then present and discuss our numerical results from the quantum simulation in comparison with analytical computations and exact diag-

onalization results in Sec. IV. Finally, our conclusions are summarized in Sec. V.

II. BACKGROUND

In this section, we first briefly introduce the $(1+1)$ -dimensional Nambu-Jona-Lasinio (NJL) model, and present the lattice discretization of the NJL Hamiltonian. Next, we provide a brief introduction of the QITE algorithm used for the quantum simulation.

A. The NJL model in $(1+1)$ dimensions

The NJL model was defined in [59, 60] with the Lagrangian density

$$\mathcal{L}_{\text{NJL}} = \bar{\psi}(i\cancel{\partial} - m)\psi + g[(\bar{\psi}\psi)^2 + (\bar{\psi}i\gamma_5\psi)^2], \quad (1)$$

where m and g represent the bare quark mass and coupling constant, respectively, and $\cancel{\partial} \equiv \gamma^\mu \partial_\mu$. The explicit representation of the $(1+1)$ -dimensional Clifford algebra $\{\gamma^\mu, \gamma^\nu\} = 2\eta^{\mu\nu}$ used in this work is

$$\gamma_0 = Z, \quad \gamma_1 = -iY, \quad \gamma_5 = \gamma_0\gamma_1 = -X \quad (2)$$

where the Pauli gates are

$$X = \begin{pmatrix} 0 & 1 \\ 1 & 0 \end{pmatrix}, \quad Y = \begin{pmatrix} 0 & -i \\ i & 0 \end{pmatrix}, \quad Z = \begin{pmatrix} 1 & 0 \\ 0 & -1 \end{pmatrix} \quad (3)$$

A simplified version of the NJL Model, the Gross-Neveu (GN) model [149], is given by

$$\mathcal{L} = \bar{\psi}(i\cancel{\partial} - m)\psi + g(\bar{\psi}\psi)^2. \quad (4)$$

To study the chiral phase transition and chirality imbalance in the GN model, we introduce additional terms related to non-zero chemical potential μ and chiral chemical potential μ_5 , which mimics the chiral imbalance between right- and left-chirality quarks coupled with the chirality charge density operator $n_5 = \bar{\psi}\gamma_0\gamma_5\psi$. Therefore, the modified Lagrangian is

$$\mathcal{L} = \bar{\psi}(i\cancel{\partial} - m)\psi + g(\bar{\psi}\psi)^2 + \mu\bar{\psi}\gamma_0\psi + \mu_5\bar{\psi}\gamma_0\gamma_5\psi. \quad (5)$$

In our previous work [148], we have studied the behavior of the chiral condensate $\langle\bar{\psi}\psi\rangle$ at $\mu_5 = 0$ with finite and non-zero temperature T and chemical potential μ . The Hamiltonian $\mathcal{H} = i\psi^\dagger\partial_0\psi - \mathcal{L}$ corresponding to Eq. (5) is given by

$$\mathcal{H} = \bar{\psi}(i\gamma_1\partial_1 + m)\psi - g(\bar{\psi}\psi)^2 - \mu\bar{\psi}\gamma_0\psi - \mu_5\bar{\psi}\gamma_0\gamma_5\psi. \quad (6)$$

For clarification, when we mention “NJL model” in this work, we refer to the Hamiltonian given in Eq. (6).

As in our previous work [148], we first use a staggered fermion field χ_{2n} , χ_{2n+1} to discretize the Dirac fermion field $\psi(x)$. With the lattice spacing a and $n = 0, \dots, N/2 - 1$ where N is an even integer, one has [150–155]

$$\psi(x) = \frac{1}{\sqrt{a}} \begin{pmatrix} \chi_{2n} \\ \chi_{2n+1} \end{pmatrix}. \quad (7)$$

Therefore, one obtains the following discrete approximations of the various operators appearing in the Hamiltonian $H = \int dx \mathcal{H}$ where periodic boundary conditions are considered,

$$\begin{aligned} \int dx \bar{\psi} i\gamma_1 \partial_1 \psi &= a \sum_{n=0}^{N/2-1} \psi_n^\dagger i\gamma_5 \partial_1 \psi_n \\ &= -\frac{i}{2a} \left[\sum_{n=0}^{N-2} \left(\chi_n^\dagger \chi_{n+1} - \chi_{n+1}^\dagger \chi_n \right) \right. \\ &\quad \left. + \left(\chi_{N-1}^\dagger \chi_0 - \chi_0^\dagger \chi_{N-1} \right) \right], \end{aligned} \quad (8)$$

$$\int dx \bar{\psi} \psi = a \sum_{n=0}^{N/2-1} \psi_n^\dagger \gamma_0 \psi_n = \sum_{n=0}^{N-1} (-1)^n \chi_n^\dagger \chi_n, \quad (9)$$

$$\begin{aligned} \int dx (\bar{\psi} \psi)^2 &= a \sum_{n=0}^{N/2-1} (\psi_n^\dagger \gamma_0 \psi_n)^2 \\ &= \frac{1}{a} \sum_{n=0}^{N/2-1} \left(\chi_{2n}^\dagger \chi_{2n} - \chi_{2n+1}^\dagger \chi_{2n+1} \right)^2 \\ &= -\frac{2}{a} \sum_{n=0}^{N/2-1} \left(\chi_{2n}^\dagger \chi_{2n} \chi_{2n+1}^\dagger \chi_{2n+1} \right) \\ &\quad + \frac{1}{a} \sum_{n=0}^{N-1} (\chi_n^\dagger \chi_n)^2, \end{aligned} \quad (10)$$

$$\int dx \bar{\psi} \gamma_0 \psi = a \sum_{n=0}^{N/2-1} \psi_n^\dagger \psi_n = \sum_{n=0}^{N-1} \chi_n^\dagger \chi_n, \quad (11)$$

$$\begin{aligned} \int dx \bar{\psi} \gamma_0 \gamma_5 \psi &= a \sum_{n=0}^{N/2-1} \psi_n^\dagger \gamma_5 \psi_n \\ &= -\sum_{n=0}^{N/2-1} \left(\chi_{2n}^\dagger \chi_{2n+1} + \chi_{2n+1}^\dagger \chi_{2n} \right). \end{aligned} \quad (12)$$

Subsequently, the Hamiltonian in Eq. (6) becomes

$$\begin{aligned} H &= \int dx [\bar{\psi} (m + i\gamma_1 \partial_1 - \mu \gamma_0 - \mu_5 \gamma_0 \gamma_5) \psi - g(\bar{\psi} \psi)^2] \\ &= m \sum_{n=0}^{N-1} (-1)^n \chi_n^\dagger \chi_n - \frac{i}{2a} \left[\sum_{n=0}^{N-2} \left(\chi_n^\dagger \chi_{n+1} - \chi_{n+1}^\dagger \chi_n \right) \right. \\ &\quad \left. + \left(\chi_{N-1}^\dagger \chi_0 - \chi_0^\dagger \chi_{N-1} \right) \right] - \mu \sum_{n=0}^{N-1} \chi_n^\dagger \chi_n \end{aligned}$$

$$\begin{aligned} &+ \mu_5 \sum_{n=0}^{N/2-1} \left(\chi_{2n}^\dagger \chi_{2n+1} + \chi_{2n+1}^\dagger \chi_{2n} \right) - \frac{g}{a} \sum_{n=0}^{N-1} (\chi_n^\dagger \chi_n)^2 \\ &+ \frac{2g}{a} \sum_{n=0}^{N/2-1} \left(\chi_{2n}^\dagger \chi_{2n} \chi_{2n+1}^\dagger \chi_{2n+1} \right)^2. \end{aligned} \quad (13)$$

In order to implement the Hamiltonian to a quantum circuit, we write down the spin representation of the Hamiltonian using the Jordan-Wigner transformation [156],

$$\chi_n = \frac{X_n - iY_n}{2} \prod_{\mu=0}^{n-1} (-iZ_\mu), \quad (14)$$

where X_n , Y_n and Z_n are the Pauli- X , Y and Z matrices acting on the n -th lattice site. In such spin representation, the discrete approximations of the relevant operators are then given by

$$\begin{aligned} \int dx \bar{\psi} i\gamma_1 \partial_1 \psi &= \sum_{n=0}^{N-2} \frac{1}{4a} (X_n X_{n+1} + Y_n Y_{n+1}) \\ &\quad + \frac{(-1)^{N/2}}{4a} (X_{N-1} X_0 + Y_{N-1} Y_0) \prod_{i=1}^{N-2} Z_i, \end{aligned} \quad (15)$$

$$\int dx \bar{\psi} \psi = \sum_{n=0}^{N-1} (-1)^n \frac{Z_n}{2}, \quad (16)$$

$$\begin{aligned} \int dx (\bar{\psi} \psi)^2 &= -\frac{1}{2a} \sum_{n=0}^{N/2-1} (\mathbb{1} + Z_{2n})(\mathbb{1} + Z_{2n+1}) \\ &\quad + \frac{1}{2a} \sum_{n=0}^{N-1} (\mathbb{1} + Z_n), \end{aligned} \quad (17)$$

$$\int dx \bar{\psi} \gamma_0 \psi = \sum_{n=0}^{N-1} \frac{Z_n}{2}, \quad (18)$$

$$\int dx \bar{\psi} \gamma_0 \gamma_5 \psi = \frac{1}{2} \sum_{n=0}^{N/2-1} (X_{2n} Y_{2n+1} - Y_{2n} X_{2n+1}). \quad (19)$$

In Eqs. (15) and (17), we have imposed periodic boundary conditions. With the relations in Eqs. (15)–(19), we decompose the total $(1+1)$ -dimensional NJL Hamiltonian into 6 pieces, writing $H = \sum_{j=1}^6 H_j$ with

$$H_1 = \sum_{n=0}^{N/2-1} \frac{1}{4a} (X_{2n} X_{2n+1} + Y_{2n} Y_{2n+1}), \quad (20)$$

$$\begin{aligned} H_2 &= \sum_{n=1}^{N/2-1} \frac{1}{4a} (X_{2n-1} X_{2n} + Y_{2n-1} Y_{2n}) \\ &\quad + \frac{(-1)^{N/2}}{4a} (X_{N-1} X_0 + Y_{N-1} Y_0) \prod_{i=1}^{N-2} Z_i, \end{aligned} \quad (21)$$

$$H_3 = \frac{m}{2} \sum_{n=0}^{N-1} (-1)^n Z_n, \quad (22)$$

$$H_4 = \frac{g}{2a} \left(\sum_{n=0}^{N/2-1} (\mathbb{1} + Z_{2n})(\mathbb{1} + Z_{2n+1}) - \sum_{n=0}^{N-1} (\mathbb{1} + Z_n) \right) \quad (23)$$

$$H_5 = -\frac{\mu}{2} \sum_{n=0}^{N-1} Z_n, \quad (24)$$

$$H_6 = -\frac{\mu_5}{2} \sum_{n=0}^{N/2-1} (X_{2n}Y_{2n+1} - Y_{2n}X_{2n+1}). \quad (25)$$

Finally, with the decomposition of the Hamiltonian shown in Eqs. (20)–(25), we are able to perform the Suzuki-Trotter decomposition [157, 158] to study the effects of the chiral chemical potential μ_5 on the finite temperature properties of the chiral condensate $\langle \bar{\psi}\psi \rangle$ and chirality charge density n_5 of the (1 + 1)-dimensional NJL model on a quantum simulator.

B. Quantum imaginary time evolution algorithm

In this section, we introduce the quantum imaginary time evolution (QITE) algorithm [159], which is used for evaluating the temperature dependence of the NJL model for various values of the baryochemical potential μ and chiral chemical potential μ_5 . As pointed out in [159], compared with other techniques for quantum thermal averaging procedures [160–163], the QITE algorithm is advantageous in generating thermal averages of observables without any ancillae or deep circuits. Moreover, the QITE algorithm is more resource-efficient and requires exponentially less space and time in each iteration than its classical equivalents.

Generally, for a given Hamiltonian H , one can approximate the (Euclidean) evolution operator $e^{-\beta H}$ by applying the Suzuki-Trotter decomposition [157, 158]

$$e^{-\beta H} = (e^{-\Delta\beta H})^N + O(\Delta\beta^2), \quad (26)$$

where $\Delta\beta$ is a chosen imaginary time step and $N = \beta/\Delta\beta$ is the number of iterations needed to reach imaginary time $\beta = 1/T$ with temperature T . However, since the evolution operator $e^{-\Delta\beta H}$ is not unitary, it cannot be implemented as a sequence of unitary quantum gates. In order to compute the Euclidean time evolution of a state $|\Psi\rangle$ on a quantum computer, one needs to approximate the action of the operator $e^{-\Delta\beta H}$ by some unitary operator. Fortunately, the QITE algorithm provides a procedure for doing this.

In the QITE algorithm, to approximate the Euclidean time evolution of $|\Psi\rangle$, a Hermitian operator A is introduced such that the effect of the non-unitary operator $e^{-\Delta\beta H}$ on a quantum state $|\Psi\rangle$ is replicated by the uni-

tary operator $e^{-i\Delta\beta A}$, namely²

$$\frac{1}{\sqrt{c(\Delta\beta)}} e^{-\Delta\beta H} |\Psi\rangle \approx e^{-i\Delta\beta A} |\Psi\rangle, \quad (27)$$

where the normalization $c(\Delta\beta) = \langle\Psi|e^{-2\Delta\beta H}|\Psi\rangle$.

When $\Delta\beta$ is very small, one is able to expand Eq. (27) up to $\mathcal{O}(\Delta\beta)$, truncating after the first nontrivial term. Then at imaginary time β , the change of the quantum states under the operators $e^{-\Delta\beta H}$ and $e^{-i\Delta\beta A}$ per small imaginary time interval $\Delta\beta$ can be represented by

$$|\Delta\Psi_H(\beta)\rangle = \frac{1}{\Delta\beta} \left(\frac{1}{\sqrt{c(\Delta\beta)}} e^{-\Delta\beta H} |\Psi(\beta)\rangle - |\Psi(\beta)\rangle \right), \quad (28)$$

$$|\Delta\Psi_A(\beta)\rangle = \frac{1}{\Delta\beta} \left(e^{-i\Delta\beta A} |\Psi(\beta)\rangle - |\Psi(\beta)\rangle \right), \quad (29)$$

As proposed in [159], to determine the Hermitian operator A , we first parameterize it in terms of Pauli matrices as below

$$A(\mathbf{a}) = \sum_{\mu} a_{\mu} \hat{\sigma}_{\mu}. \quad (30)$$

Here $\hat{\sigma}_{\mu} = \prod_l \sigma_{\mu_l, l}$ is a Pauli string and the subscript μ of a_{μ} labels the various Pauli strings. To evaluate the Hermitian operator A , we need to minimize the objective function $F(a)$ defined by

$$\begin{aligned} F(a) &= \|(|\Delta\Psi_H(\beta)\rangle - |\Delta\Psi_A(\beta)\rangle)\|^2 \\ &= \| |\Delta\Psi_H(\beta)\rangle \|^2 + \sum_{\mu, \nu} a_{\nu} a_{\mu} \langle\Psi(\beta)| \hat{\sigma}_{\nu}^{\dagger} \hat{\sigma}_{\mu} |\Psi(\beta)\rangle \\ &\quad + i \sum_{\mu} \frac{a_{\mu}}{\sqrt{c(\Delta\beta)}} \langle\Psi(\beta)| (H \hat{\sigma}_{\mu} - \hat{\sigma}_{\mu}^{\dagger} H) |\Psi(\beta)\rangle. \end{aligned} \quad (31)$$

The first term $\| |\Delta\Psi_H(\beta)\rangle \|^2$ is irrelevant to a_{μ} . Thus, we take the derivative with respect to a_{μ} and set it equal to zero, yielding the linear equation $(\mathbf{S} + \mathbf{S}^T) \mathbf{a} = \mathbf{b}$, where the matrix \mathbf{S} and vector \mathbf{b} are defined by

$$S_{\mu\nu} = \langle\Psi(\beta)| \hat{\sigma}_{\nu}^{\dagger} \hat{\sigma}_{\mu} |\Psi(\beta)\rangle, \quad (32)$$

$$b_{\mu} = -\frac{i}{\sqrt{c(\Delta\beta)}} \langle\Psi(\beta)| (H \hat{\sigma}_{\mu} - \hat{\sigma}_{\mu}^{\dagger} H) |\Psi(\beta)\rangle. \quad (33)$$

From this equation, we are able to solve for a_{μ} and evolve an initial quantum state under the unitary operator $e^{-i\Delta\beta A}$ to any imaginary time β by Trotterization,

$$|\Psi(\beta)\rangle = (e^{-i\Delta\beta A})^N |\Psi(0)\rangle + \mathcal{O}(\Delta\beta). \quad (34)$$

In the remainder of this section, we compare the performance of the QITE algorithm to the Variational Quantum

² Recall that quantum states are represented by rays $\{\alpha|\Psi\rangle : \alpha \in \mathbb{C}\}$ in a Hilbert state, not by the vectors themselves, since the normalization/phase of the state vectors are nonphysical.

Eigensolver (**VQE**) algorithms in obtaining the ground-state energy of the (1+1)-dimensional NJL model defined above. As pointed out in [159], the **QITE** algorithm is efficient for calculating ground-state energies. In Fig. 1, we plot the ground-state energy with bare mass $m = 100$ MeV, chemical potentials $\mu = 100$ MeV and $\mu_5 = 10$ MeV at $g = 1$ and $g = 5$, respectively, as a function of the number of operation steps performed by the various algorithms. The **VQE** algorithms have been used to obtain many stellar results on NISQ hardware [164–167], sparking a lot of attention recently. However, the reliance on an ansatz limits the effectiveness of the algorithm, as the part of the Hilbert space that the **VQE** can scan is influenced by the specific variational ansatz used, and the classical component of the algorithm requires optimization as well. The **QITE** algorithm, on the other hand, does not need an ansatz and evolves the prepared state closer to the ground state after each time-step in a controlled manner. The state should converge to the ground state provided the initial state has some overlap with it, with a *quantifiable* error.

As presented in Fig. 1, we plot 500 operation steps for both **QITE** (blue points with curve) and **VQE** algorithms (light-blue, green and orange curves for various optimizers). For the **QITE** algorithm, we chose imaginary time step $\Delta\beta = 0.001$ and the quantum circuit is implemented in **QFORTE** [168], a quantum algorithms library based on **PYTHON**. For the **VQE** algorithm, operation steps are the optimizer steps and the results are given by **QISKIT** [169] of **IBMQ** [170], where various optimizers are applied for comparison with **QITE** simulations. One can find that the **QITE** algorithm reaches the ground-state energy at a higher accuracy in less operation steps compared to the optimizers of **VQE** shown in the plot. In fact, one can see that the error of the **VQE** implementations “levels off” at around 1%, a consequence of the variational ansatz scanning a set that is a finite distance from the true vacuum.

Besides calculating the ground state energy, another powerful application of the **QITE** algorithm is to simulating the temperature dependence of a thermal process. In this work, we will use the **QITE** algorithm introduced above to generate the thermal state $|\Psi(\beta/2)\rangle$, then apply the following relation to obtain the thermal average of an observable \hat{O} ,

$$\langle \hat{O} \rangle_\beta = \frac{\text{Tr}(e^{-\beta \hat{H}} \hat{O})}{\text{Tr}(e^{-\beta \hat{H}})} = \frac{\sum_{i \in \mathcal{S}} \langle i | e^{-\beta \hat{H}/2} \hat{O} e^{-\beta \hat{H}/2} | i \rangle}{\sum_{i \in \mathcal{S}} \langle i | e^{-\beta \hat{H}} | i \rangle}. \quad (35)$$

Here \mathcal{S} is a complete set as the basis of the ground state [159]. Specifically, we will choose $\hat{O} = \bar{\psi}\psi$ and $\hat{O} = \bar{\psi}\gamma_0\gamma_5\psi$ for calculating the thermal average of chiral condensate $\langle\bar{\psi}\psi\rangle$ and chirality charge density $n_5 = \langle\bar{\psi}\gamma_0\gamma_5\psi\rangle$.

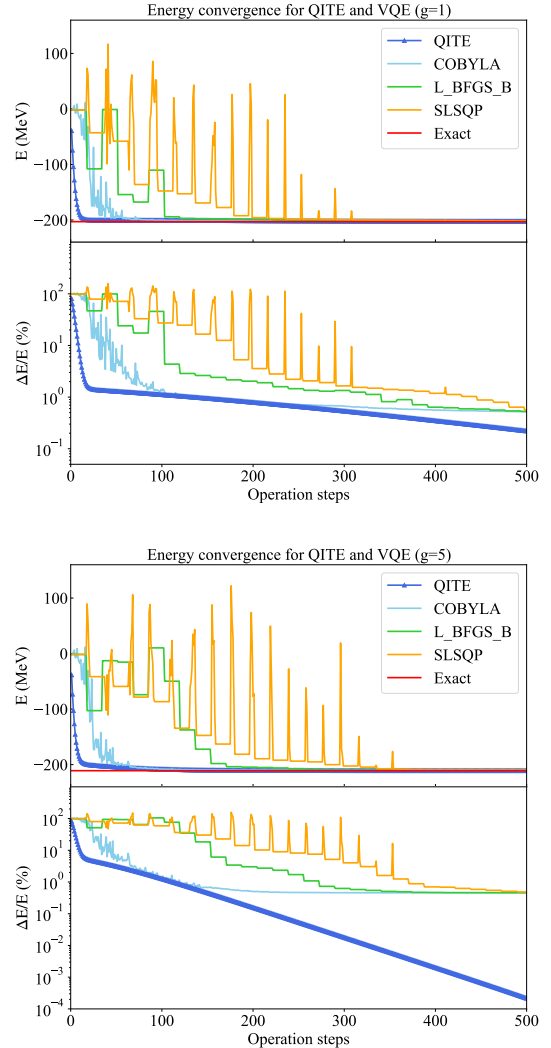


FIG. 1. Comparison between the **QITE** algorithms and **VQE** of various optimizers (**COBYLA**, **L_BFGS_B** and **SLSQP**) for $g = 1$ (top panel) and $g = 5$ (bottom panel) to reach the ground state energy of the NJL Hamiltonian. We use 4 qubits for the NJL model with $m = 100$ MeV, $g = 1$, $\mu = 100$ MeV and $\mu_5 = 10$ MeV. For the **VQE** algorithm, the x -axis represents the number of optimization steps while for the **QITE** algorithms, the x -axis is the number of thermal evolution steps $x = \beta/\Delta\beta$ ($\Delta\beta = 0.001$). We chose three optimizers provided by **QISKIT** and set the maximum optimization steps as 500 for all optimizers.

III. ANALYTICAL CALCULATION

In this section, before reaching out to quantum simulations, we first provide the analytical calculations for the chiral condensate and chirality charge density at finite temperature T , baryochemical potential μ and chiral chemical potential μ_5 using the Lagrangian provided in Eq. (5) by minimizing the thermodynamic (Landau) potential.

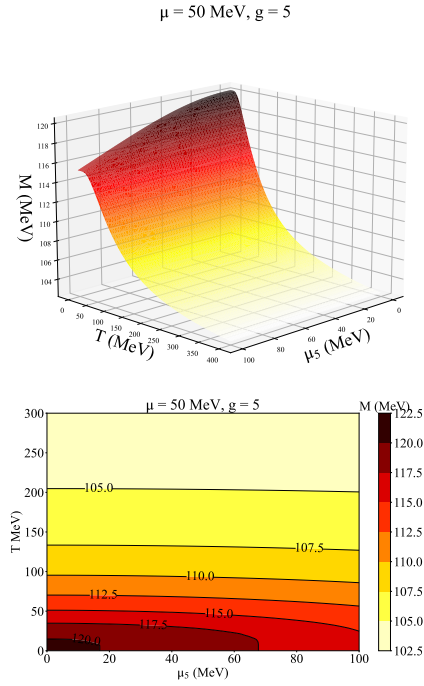


FIG. 2. The effective mass M as a function of the chiral chemical potential μ_5 and temperature T at $g = 5$, chemical potential $\mu = 50$ MeV. Upper: 3D Surface Plot. Lower: Contour Plot.

A. The Landau potential and chiral condensate

We first provide theoretical calculations for the vacuum chiral condensate $\langle\bar{\psi}\psi\rangle$ at various temperatures T , chemical potentials μ and μ_5 under the Hamiltonian \mathcal{H} as defined in Eq. (6). The chiral condensate $\langle\bar{\psi}\psi\rangle$, known to be an order parameter [171–175] for the chiral phase transition in the chiral limit ($m \sim 0$), has been studied in the *mean field* approximation. That is to say, as introduced in [149, 176], one writes $\bar{\psi}\psi = \langle\bar{\psi}\psi\rangle + \sigma$ with a constant³ term $\langle\bar{\psi}\psi\rangle$ and a small real scalar field σ , corresponding to fluctuations about the vacuum value, and then drop terms that are $\mathcal{O}(\sigma^2)$. Then the four-fermion contact interaction $g(\bar{\psi}\psi)^2$ can be written as

$$\begin{aligned} g(\bar{\psi}\psi)^2 &= g(\langle\bar{\psi}\psi\rangle + \sigma)^2 \\ &= 2g\bar{\psi}\psi\langle\bar{\psi}\psi\rangle - g\langle\bar{\psi}\psi\rangle^2 + \mathcal{O}(\sigma^2). \end{aligned} \quad (36)$$

Furthermore, by defining the effective mass $M(\mu, \mu_5, T)$

$$M(\mu, \mu_5, T) = m - 2g\langle\bar{\psi}\psi\rangle(\mu, \mu_5, T), \quad (37)$$

the Lagrangian is given by $\mathcal{L} = \mathcal{L}_{\text{eff}} + \mathcal{O}(\sigma^2)$, where

$$\begin{aligned} \mathcal{L}_{\text{eff}} &= \bar{\psi}(i\partial - M + \mu\gamma_0 + \mu_5\gamma_0\gamma_5)\psi - \frac{(M - m)^2}{4g} \\ &= \mathcal{L}_{\text{Dirac}} - \mathcal{V}, \end{aligned} \quad (38)$$

where the potential \mathcal{V} is related to the chiral condensate as well as the effective mass

$$\mathcal{V} = g\langle\bar{\psi}\psi\rangle^2 = (M - m)^2/4g. \quad (39)$$

Following [2, 77], the Grand Canonical Potential Ω_{Dirac} of $\mathcal{L}_{\text{Dirac}}$ with mass M is given in the following form

$$\begin{aligned} \Omega_{\text{Dirac}}(\mu, \mu_5, T; M) &= -\frac{2}{\pi} \sum_{s=\pm 1} \int_0^\infty \left[T \ln(1 + e^{-\beta(\omega_{k,s} + \mu)}) \right. \\ &\quad \left. + T \ln(1 + e^{-\beta(\omega_{k,s} - \mu)}) + \omega_{k,s} \right] dk, \end{aligned} \quad (40)$$

where the energy spectrum of the free fermions $\omega_{k,s} = \sqrt{(k + s\mu_5)^2 + M^2}$ with $s = \pm 1$. Then, by adding the potential $\mathcal{V} = (M - m)^2/4g$, we obtain the grand canonical potential for the NJL model as follows

$$\begin{aligned} \Omega(\mu, \mu_5, T; M) &= \mathcal{V} - \frac{2}{\pi} \sum_s \int_0^\infty \left[T \ln(1 + e^{-\beta(\omega_{k,s} + \mu)}) \right. \\ &\quad \left. + T \ln(1 + e^{-\beta(\omega_{k,s} - \mu)}) + \omega_{k,s} \right] dk. \end{aligned} \quad (41)$$

Due to the divergent behavior of this quantity, one has to regularize it. In this work, for comparison with numerical results with the lattice spacing a , the natural momentum cutoff is $\Lambda = \pi/a$. With this hard momentum cutoff imposed for the integral shown in Eq. (41), one is able to determine the effective mass M at fixed values of μ , μ_5 and T numerically by minimizing $\Omega(\mu, \mu_5, T; M)$ in regard to M , namely solving the gap equation,

$$\frac{\partial \Omega(\mu, \mu_5, T; M)}{\partial M} = 0. \quad (42)$$

Then the chiral condensate is given by $\langle\bar{\psi}\psi\rangle = (m - M)/2g$ following Eq. (37).

As an example, in Fig. 2, we present the effective mass M plot as a function of temperature T and chiral chemical potential μ_5 with bare mass $m = 100$ MeV, coupling constant $g = 5$, lattice spacing $a = 1$ MeV⁻¹ and chemical potential $\mu = 50$ MeV. As expected, at high μ_5 or T , one has $M \rightarrow m$, corresponding to a restoration of chiral symmetry. Conversely, at low $(\mu_5^2 + T^2)$, one finds a dynamically generated mass of around $\Delta m \equiv M - m \sim 20$ MeV. Therefore, a free field theory is expected at asymptotically high temperatures/chemical potentials [149].

B. The chirality charge density

In a magnetic field, under the imbalance of right/left-handed chirality, a finite induced current is produced

³ Here “constant” means unchanged with the coordinates. $\langle\bar{\psi}\psi\rangle$, known as the *global* chiral condensate [177, 178], is coordinate-independent and distinguished from the *local* chiral condensate $\langle\bar{\psi}(x)\psi(x)\rangle$ which depend on the coordinates. De facto, $\langle\bar{\psi}\psi\rangle$ is a function of temperature T and chemical potentials μ and μ_5 .

along the magnetic field. Specifically, when the number of right-handed quarks, N_R is unequal to that of the left-handed quarks N_L , positive charge is separated from negative charge along the magnetic field, which is the so-called “Chiral Magnetic Effect” [28–30]. The axial anomaly and topological objects in QCD are the fundamental physics of the CME. Unbalanced left- and right-handed quarks can produce observable effects that can be used to investigate topological \mathcal{P} - and \mathcal{CP} -odd excitations [36–39].

In Eq. (5), we have introduced an additional term with the chiral chemical potential μ_5 coupled with the chirality charge density operator $n_5 = \bar{\psi}\gamma_0\gamma_5\psi$, which has been known as a distinctive characteristic in hot and dense QCD matter and is not conserved as a consequence of the chiral anomaly. In the presence of a chiral chemical potential μ_5 , a manifestation of the chiral imbalance, the non-vanishing finite chirality charge density n_5 is required for the CME effect and recognized as a unique property of hot and dense QCD matter. Despite the fact that the chiral chemical potential μ_5 is introduced for studying topological charge fluctuations, it is considered as a time-independent quantity that represents the chiral imbalance. And the chirality charge density $n_5 = \langle\bar{\psi}\gamma_0\gamma_5\psi\rangle$ is a constant in the coordinates like the chiral condensate $\langle\bar{\psi}\psi\rangle$ ⁴.

When describing the induced electric current density as a function of the chirality density, the relationship between n_5 and μ_5 is important and the chirality charge density n_5 can be calculated by [1]

$$n_5 = -\frac{\partial\Omega(\mu, \mu_5, T; M)}{\partial\mu_5}, \quad (43)$$

where the grand potential $\Omega(\mu, \mu_5, T; M)$ is given in Eq. (41). In the next section, we will present the analytical calculations of n_5 in comparison with QITE and exact diagonalization results.

IV. RESULTS

In this subsection, we study the finite temperature behaviors of the chiral condensate $\langle\bar{\psi}\psi\rangle$ and chirality charge density $n_5 = \langle\bar{\psi}\gamma_0\gamma_5\psi\rangle$ in the (1 + 1)-dimensional NJL model given in Eq. (13). As emphasized in previous sections, we apply a quantum algorithm to simulate the thermal behaviours of physical observables. To demonstrate the reliability of our simulations, we will provide all the result from three different approaches:

1. QITE simulations of the thermal observable;

2. Exact diagonalizations from the discretization of the NJL Hamiltonian;
3. Analytical calculations given by solving the gap equation numerically.

For the consistency among the three procedures, we have chosen the same bare mass $m = 100$ MeV and lattice spacing $a = 1$ MeV^{−1}. The coupling constant g at $g = 1$ and $g = 5$ are applied for testing the effects of the four-fermion interaction term in the Lagrangian.

To apply the quantum circuits, many quantum simulation packages have been developed and give similar results for quantum simulations. These quantum simulators, such as PYQUILL [179] (Rigetti), TEQUILA [180], Q# [181] (Microsoft), QISKIT [182] (IBM), QFORTE [168], XACC [183], FQE [184] CIRQ [185], are PYTHON software libraries and the outputs are the expected outputs of an ideal quantum computer. One can find a list of general quantum simulation packages in [186] and some implementations of the quantum algorithms are listed in [187]. To execute the QITE algorithm, we construct a quantum circuit using the open-source software package QFORTE [168], where many useful quantum algorithms have been implemented.

A. Chiral condensate

To study the effects of the chiral imbalance on the chiral condensate at finite temperatures and chemical potentials, we present plots of the effective mass M at various chemical potentials μ , μ_5 and temperatures T in Figs. 3, 4 and 5, respectively. In Fig. 3, we compare the temperature dependence of the effective mass M at $g = 1$ and $g = 5$ as a function of temperature T at chiral chemical potential $\mu_5 = 0, 10, 30$ and 50 MeV with a fixed baryochemical potentials $\mu \in \{0, 50, \dots, 250\}$ MeV in each panel, where filled diamond points are given by the QITE algorithm, hollow circle points are from exact diagonalization and solid curve results are calculated analytically. Between $\mu = 100$ MeV and $\mu = 150$ MeV panels, the pattern of the effective mass changed from decreasing ($\mu \leq 100$ MeV) to increasing with temperature ($\mu \geq 150$ MeV). Also for $\mu \leq 100$ MeV panels, the effective mass M at smaller μ_5 is larger, while for $\mu \geq 150$ MeV panels, the effective mass M at smaller μ_5 is smaller.

In Fig. 4, we fix the value of chiral chemical potentials μ_5 in each panel and plot the $M-T$ curves at various baryochemical potentials $\mu = 0, 50, \dots, 250$ MeV at $g = 1$ and $g = 5$. A non-trivial phase transition at $100 < \mu < 150$ MeV is observed in all the panels and this has also been pointed out when interpreting Fig. 4. The patterns look similar at various μ_5 and we find that at smaller μ_5 , the effective mass M changes more rapidly as a function of T .

To better illustrate the effects of μ_5 , we present the effective mass M as a function of chiral chemical poten-

⁴ Here the coordinate-independent chirality charge density $n_5 = \langle\bar{\psi}\gamma_0\gamma_5\psi\rangle$ is also a *global* quantity, like the *global* chiral condensate defined in [177, 178] and it will depend on the temperature T and the chemical potentials μ and μ_5 .

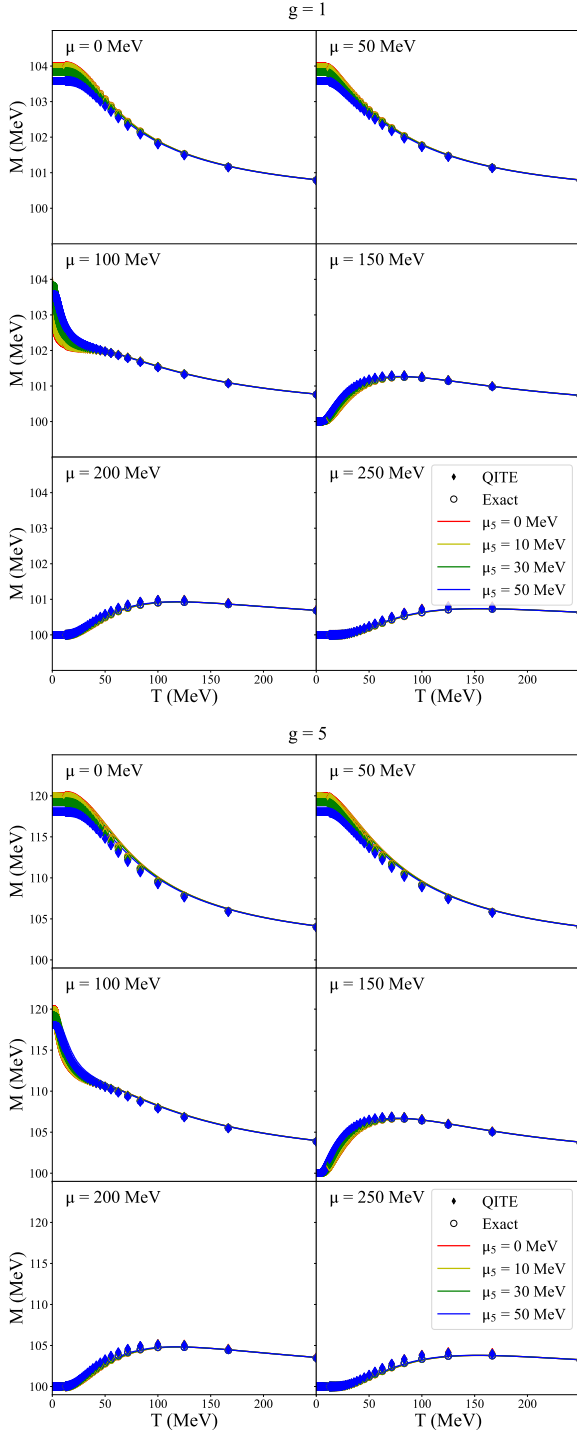


FIG. 3. Chiral Condensate $\langle\bar{\psi}\psi\rangle$ as a function of temperature T MeV at coupling constant $g = 1$ (top panel) and $g = 5$ (bottom panel) with a fixed chemical potential μ in each panel. Filled diamond points are given by QITE algorithm, hollow circle points are from exact diagonalization and solid curves are calculated analytically.

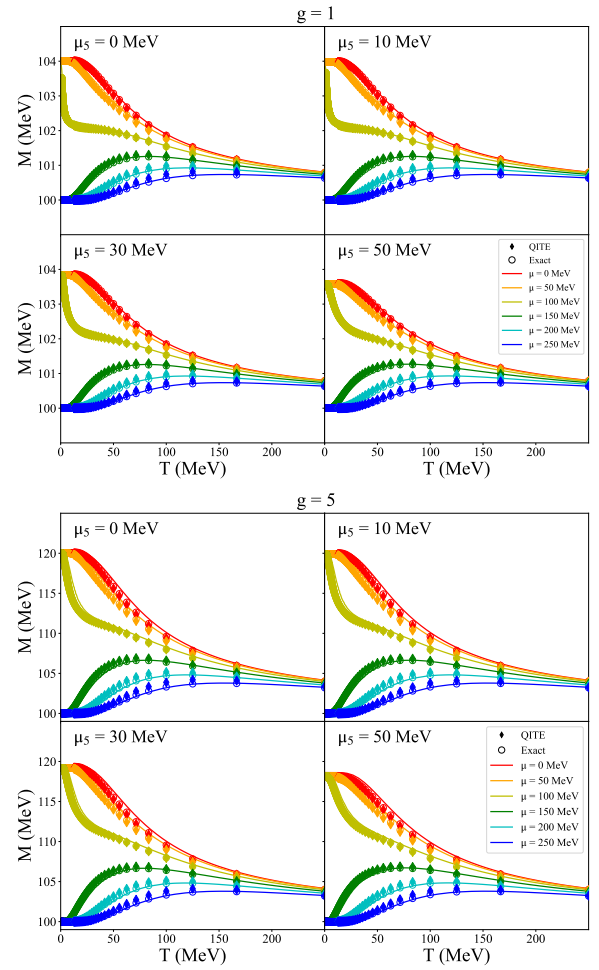


FIG. 4. Chiral Condensate $\langle\bar{\psi}\psi\rangle$ as a function of temperature T MeV at coupling constant $g = 1$ (top panel) and $g = 5$ (bottom panel) at a fixed chiral chemical potential μ_5 in each panel.

tials μ_5 and show the results at several temperatures and baryochemical potentials in Fig. 5 for $g = 1$ and $g = 5$. The effective mass changes slightly as the chiral chemical potential increases, indicating that the chiral chemical potential plays a lesser role in chiral symmetry breaking than the temperature and chemical potential, at least in this model. At $\mu \leq 100$ MeV, M is lower for higher temperature, which is expected by the asymptotic freedom. While as μ increases, the effective mass M becomes smaller at lower temperatures.

B. Chirality charge density

In this subsection, we present the results for the chirality charge density n_5 using the QITE algorithm in comparison with analytical calculations as introduced in Sec. III B and exact diagonalization.

In Fig. 6, we plot the chirality charge density as a function of temperature T at coupling constant $g = 1$

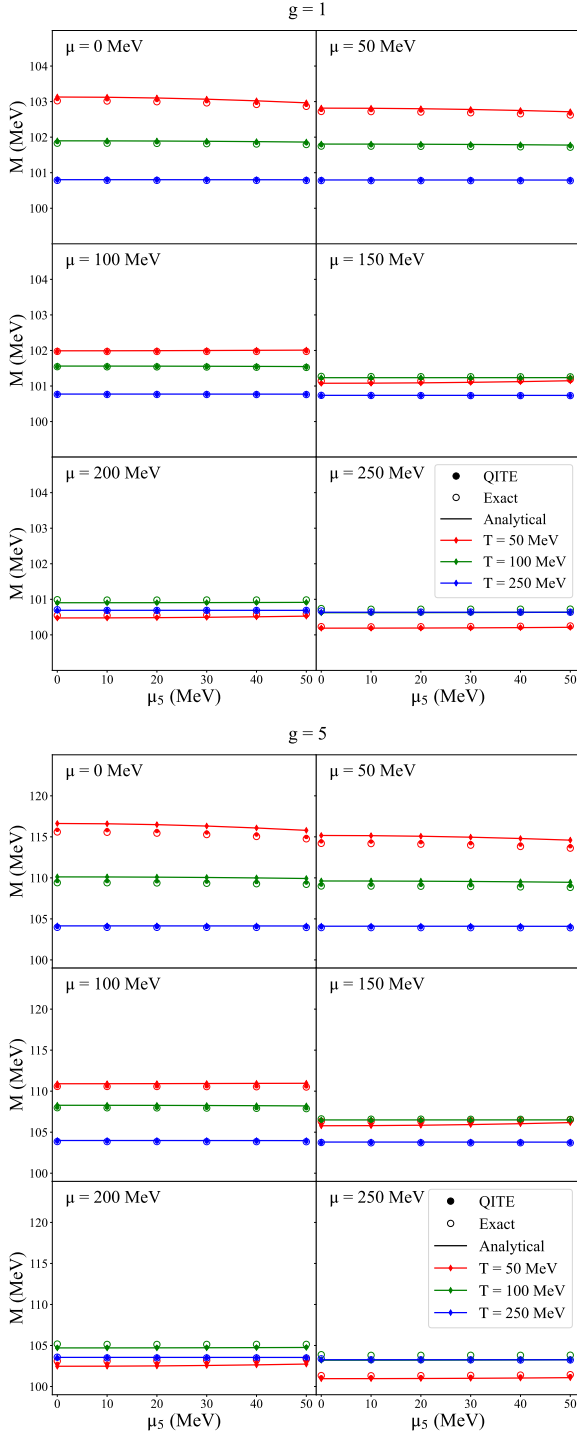


FIG. 5. Chiral Condensate $\langle\bar{\psi}\psi\rangle$ as a function of μ_5 at coupling constant $g = 1$ (top panel) and $g = 5$ (bottom panel).

and $g = 5$. We use different colors to distinguish various chiral chemical potentials $\mu_5 = 0, 10, 30$ and 50 MeV and in each panel, the chemical potential μ is fixed at $0, 50, 100, \dots$ or 250 MeV. At $\mu_5 = 0$ MeV, one obtains $n_5 = 0$ since there is no other mechanism for generating a nonzero $\mathcal{N}_5 = \bar{\psi}\gamma_0\gamma_5\psi = \psi_R^\dagger\psi_R - \psi_L^\dagger\psi_L$. As a result,

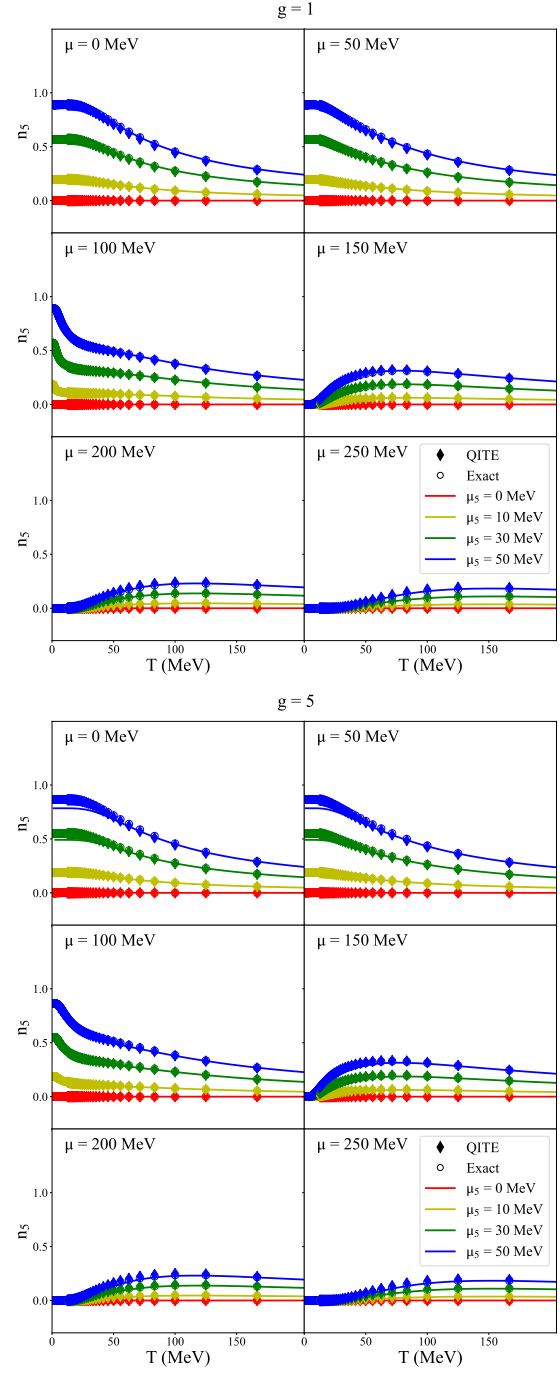


FIG. 6. Chirality charge density n_5 as a function of temperature T at $g = 1$ (top panel) and $g = 5$ (bottom panel) at a fixed chemical potential $\mu = 0, 50, 100, \dots, 250$ MeV in each panel.

only when $\mu_5 \neq 0$, there exists non-zero $n_5 = \langle\mathcal{N}_5\rangle$.

Similar to what was observed in the effective mass plots in Fig. 3, a non-trivial phase transition is observed between $\mu = 100$ MeV and $\mu = 150$ MeV. For $\mu \leq 100$ MeV, the chirality charge density decreases as temperature rises, while for $\mu \geq 150$ MeV, the chirality charge density first increases then drops and converges to 0 with

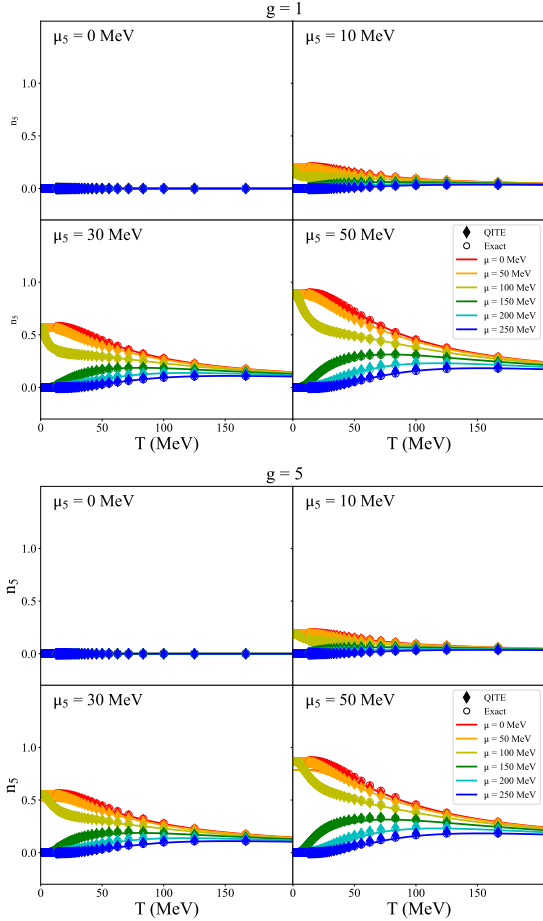


FIG. 7. Chirality charge density n_5 as a function of temperature at $g = 1$ (top panel) and $g = 5$ (bottom panel) with a fixed chiral chemical potential μ_5 in each panel.

the increasing of temperature.

In Fig. 7, we plot the chirality charge density n_5 as a function of temperature T at coupling constants $g = 1$ and $g = 5$. We use different colors to distinguish various chemical potentials $\mu \in \{0, 50, \dots, 250\}$ MeV and in each panel, the chemical potential μ_5 is fixed at 0, 10, 30 or 50 MeV. At $\mu_5 = 0$ MeV, the chirality charge density is 0 at all temperatures and chemical potentials, as expected from the previous figure. At non-zero μ_5 values, the phase transition between $\mu = 100$ MeV and $\mu = 150$ MeV can also be observed: for $\mu \leq 100$ MeV, the chirality charge density begins at some non-zero value at $T = 0$ MeV and decreases with temperature, while for curves $\mu \geq 150$ MeV, the chirality charge density begins at 0 at $T = 0$ MeV and first increases before decreasing and converging to 0 with increasing temperature. At greater values of μ_5 , curves with $\mu \leq 100$ MeV begin at higher chirality charge densities.

In Fig. 8, we plot the chirality charge density n_5 as a function of chiral chemical potential μ_5 at coupling constants $g = 1$ and $g = 5$. Colors are used to distinguish between different various temperatures $T = 50, 100,$

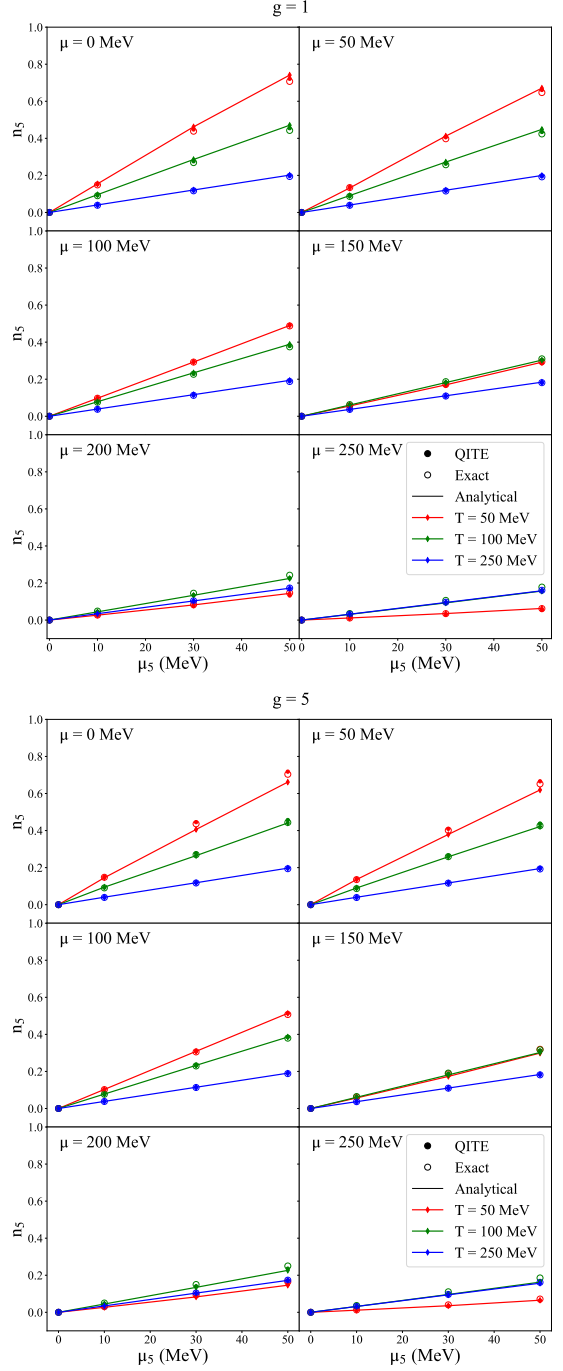


FIG. 8. Chirality charge density n_5 as a function of chiral chemical potential μ_5 at $g = 1$ (top panel) and $g = 5$ (bottom panel) with a fixed temperature T in each panel.

or 200 MeV, and the chemical potential is fixed at $\mu = 0, 50, \dots, 250$ MeV in each panel. At all chemical potentials μ and temperatures T , we see that (approximately) $n_5 \propto \mu_5$: the chirality charge density n_5 begins at 0 MeV at $\mu_5 = 0$ MeV, and increases linearly with μ_5 . The chiral chemical potential μ_5 , at least in this model, is thus a direct measure of chiral imbalance in the plasma.

Higher chemical potentials μ result in a slower increase of n_5 with μ_5 . Once again, a phase transition can be observed between $\mu \leq 100$ MeV and $\mu \geq 150$ MeV. For $\mu \leq 100$ MeV, at each μ_5 , n_5 decreases with increasing temperature. For $\mu \geq 150$ MeV, n_5 first increases with temperature from $T = 50$ MeV to $T = 100$ MeV, but then decreases from $T = 100$ MeV to $T = 200$ MeV.

V. CONCLUSION

In conclusion, using the QITE algorithm, we performed a quantum simulation for the chiral phase transition of the 1+1 dimensional NJL model at finite temperature, baryochemical potential and chiral chemical potential. Specifically, we use a 4-qubit quantum circuit to simulate the NJL Hamiltonian and find that the results among the digital quantum simulation, exact diagonalization, and analytical analysis are all consistent, implying that quantum computing will be a promising tool in simulating finite-temperature behaviors in the future for QCD.

The quantum simulations' efficacy has been shown to be insensitive to the chemical potentials μ and μ_5 (and possibly other external parameters), which opens up new

possibilities for studying finite density effects in QCD and other field theories. Owing to technological constraints (nonperturbative dynamics, Monte Carlo failure due to the sign problem, etc.) restricting the use of typical computing methods, this element of quark physics remains substantially unexplored in comparison to other fields. With the development of scalable quantum computing technologies on the horizon, Lattice QCD calculations on quantum computers are becoming not only conceivable, but also practical.

This research, together with prior research, shows that NISQ quantum computers may produce consistent and correct answers to physical issues that cannot be solved efficiently or effectively using classical computing algorithms, reflecting bright prospects for future applications of quantum computing to non-perturbative QCD in the NISQ era and beyond.

ACKNOWLEDGEMENTS

We thank Henry Ma for discussions and collaborations at early stages of this work. This work is supported by the National Science Foundation under grant No. PHY-1945471.

-
- [1] K. Fukushima, M. Ruggieri, and R. Gatto, *Phys. Rev. D* **81**, 114031 (2010), arXiv:1003.0047 [hep-ph].
 - [2] M. Buballa, *Phys. Rept.* **407**, 205 (2005), arXiv:hep-ph/0402234.
 - [3] L. McLerran and R. D. Pisarski, *Nucl. Phys. A* **796**, 83 (2007), arXiv:0706.2191 [hep-ph].
 - [4] L. McLerran, K. Redlich, and C. Sasaki, *Nucl. Phys. A* **824**, 86 (2009), arXiv:0812.3585 [hep-ph].
 - [5] D. P. Menezes, M. B. Pinto, S. S. Avancini, A. P. Martínez, and C. Providência, *Phys. Rev. C* **79**, 035807 (2009).
 - [6] M. Orsaria, H. Rodrigues, F. Weber, and G. A. Contrera, *Phys. Rev. C* **89**, 015806 (2014), arXiv:1308.1657 [nucl-th].
 - [7] M. Ruggieri and G. X. Peng, *Phys. Rev. D* **93**, 094021 (2016), arXiv:1602.08994 [hep-ph].
 - [8] J. C. Jiménez, *Interacting quark matter effects on the structure of compact stars*, Other thesis (2021), arXiv:2104.03551 [hep-ph].
 - [9] M. Gyulassy and L. McLerran, *Nucl. Phys. A* **750**, 30 (2005), arXiv:nucl-th/0405013.
 - [10] O. Soloveva, D. Fuseau, J. Aichelin, and E. Bratkovskaya, *Phys. Rev. C* **103**, 054901 (2021), arXiv:2011.03505 [nucl-th].
 - [11] K. Fukushima and T. Hatsuda, *Rept. Prog. Phys.* **74**, 014001 (2011), arXiv:1005.4814 [hep-ph].
 - [12] S. Choudhury *et al.*, *Chin. Phys. C* **46**, 014101 (2022), arXiv:2105.06044 [nucl-ex].
 - [13] Y. Feng, J. Zhao, H. Li, H.-j. Xu, and F. Wang, *Phys. Rev. C* **105**, 024913 (2022), arXiv:2106.15595 [nucl-ex].
 - [14] M. Abdallah *et al.* (STAR), *Phys. Rev. C* **105**, 014901 (2022), arXiv:2109.00131 [nucl-ex].
 - [15] R. Milton, G. Wang, M. Sergeeva, S. Shi, J. Liao, and H. Z. Huang, *Phys. Rev. C* **104**, 064906 (2021), arXiv:2110.01435 [nucl-th].
 - [16] D. E. Kharzeev, J. Liao, and S. Shi, (2022), arXiv:2205.00120 [nucl-th].
 - [17] D. E. Kharzeev (2022) arXiv:2204.10903 [hep-ph].
 - [18] P. Adhikari, *Nucl. Phys. B* **974**, 115627 (2022), arXiv:2111.06196 [hep-ph].
 - [19] A. N. Tawfik and A. M. Diab, *Eur. Phys. J. A* **57**, 200 (2021), arXiv:2106.04576 [hep-ph].
 - [20] G. Cao, *Eur. Phys. J. A* **57**, 264 (2021), arXiv:2103.00456 [hep-ph].
 - [21] J. a. Moreira, P. Costa, and T. E. Restrepo, *Eur. Phys. J. A* **57**, 123 (2021), arXiv:2101.12004 [hep-ph].
 - [22] H. T. Ding, S. T. Li, A. Tomiya, X. D. Wang, and Y. Zhang, *Phys. Rev. D* **104**, 014505 (2021), arXiv:2008.00493 [hep-lat].
 - [23] J. Zhao and F. Wang, *Prog. Part. Nucl. Phys.* **107**, 200 (2019), arXiv:1906.11413 [nucl-ex].
 - [24] A. N. Tawfik, A. M. Diab, and M. T. Hussein, *Chin. Phys. C* **43**, 034103 (2019), arXiv:1901.03293 [hep-ph].
 - [25] V. P. Gusynin, V. A. Miransky, and I. A. Shovkovy, *Nucl. Phys. B* **563**, 361 (1999), arXiv:hep-ph/9908320.
 - [26] K. G. Klimenko, *Teor. Mat. Fiz.* **89**, 211 (1991).
 - [27] S. P. Klevansky and R. H. Lemmer, *Phys. Rev. D* **39**, 3478 (1989).
 - [28] D. Kharzeev and A. Zhitnitsky, *Nucl. Phys. A* **797**, 67 (2007), arXiv:0706.1026 [hep-ph].
 - [29] D. E. Kharzeev, L. D. McLerran, and H. J. Warringa, *Nucl. Phys. A* **803**, 227 (2008), arXiv:0711.0950 [hep-ph].

- [30] K. Fukushima, D. E. Kharzeev, and H. J. Warringa, *Phys. Rev. D* **78**, 074033 (2008), arXiv:0808.3382 [hep-ph].
- [31] D. Diakonov, *Prog. Part. Nucl. Phys.* **51**, 173 (2003), arXiv:hep-ph/0212026.
- [32] T. Schäfer and E. V. Shuryak, *Phys. Rev. D* **53**, 6522 (1996), arXiv:hep-ph/9509337.
- [33] P. B. Arnold and L. D. McLerran, *Phys. Rev. D* **37**, 1020 (1988).
- [34] M. Fukugita and T. Yanagida, *Phys. Rev. D* **42**, 1285 (1990).
- [35] L. D. McLerran, E. Mottola, and M. E. Shaposhnikov, *Phys. Rev. D* **43**, 2027 (1991).
- [36] E. Witten, *Nucl. Phys. B* **156**, 269 (1979).
- [37] G. Veneziano, *Nucl. Phys. B* **159**, 213 (1979).
- [38] T. Schäfer and E. V. Shuryak, *Rev. Mod. Phys.* **70**, 323 (1998), arXiv:hep-ph/9610451.
- [39] E. Vicari and H. Panagopoulos, *Phys. Rept.* **470**, 93 (2009), arXiv:0803.1593 [hep-th].
- [40] D. E. Kharzeev, J. Liao, S. A. Voloshin, and G. Wang, *Prog. Part. Nucl. Phys.* **88**, 1 (2016), arXiv:1511.04050 [hep-ph].
- [41] A. Bzdak, S. Esumi, V. Koch, J. Liao, M. Stephanov, and N. Xu, *Phys. Rept.* **853**, 1 (2020), arXiv:1906.00936 [nucl-th].
- [42] B.-X. Chen and S.-Q. Feng, *Chin. Phys. C* **44**, 024104 (2020), arXiv:1909.10836 [hep-ph].
- [43] S. A. Voloshin, *Phys. Rev. C* **70**, 057901 (2004), arXiv:hep-ph/0406311.
- [44] B. I. Abelev *et al.* (STAR), *Phys. Rev. C* **81**, 054908 (2010), arXiv:0909.1717 [nucl-ex].
- [45] B. I. Abelev *et al.* (STAR), *Phys. Rev. Lett.* **103**, 251601 (2009), arXiv:0909.1739 [nucl-ex].
- [46] Y. Hu (STAR), *EPJ Web Conf.* **259**, 13013 (2022), arXiv:2110.15937 [nucl-ex].
- [47] M. Abdallah *et al.* (STAR), *Phys. Rev. Lett.* **128**, 092301 (2022), arXiv:2106.09243 [nucl-ex].
- [48] J. Zhao (STAR), *Nucl. Phys. A* **1005**, 121766 (2021), arXiv:2002.09410 [nucl-ex].
- [49] B. Abelev *et al.* (ALICE), *Phys. Rev. Lett.* **110**, 012301 (2013), arXiv:1207.0900 [nucl-ex].
- [50] J. Adam *et al.* (ALICE), *Phys. Rev. C* **93**, 044903 (2016), arXiv:1512.05739 [nucl-ex].
- [51] S. Parmar (ALICE), *Springer Proc. Phys.* **203**, 785 (2018), arXiv:1703.09496 [hep-ex].
- [52] S. Acharya *et al.* (ALICE), *Phys. Lett. B* **777**, 151 (2018), arXiv:1709.04723 [nucl-ex].
- [53] S. Acharya *et al.* (ALICE), *JHEP* **09**, 160 (2020), arXiv:2005.14640 [nucl-ex].
- [54] A. M. Sirunyan *et al.* (CMS), *Phys. Rev. C* **97**, 044912 (2018), arXiv:1708.01602 [nucl-ex].
- [55] V. Khachatryan *et al.* (CMS), *Phys. Rev. Lett.* **118**, 122301 (2017), arXiv:1610.00263 [nucl-ex].
- [56] D. E. Kharzeev and Y. Kikuchi, *Phys. Rev. Res.* **2**, 023342 (2020), arXiv:2001.00698 [hep-ph].
- [57] M. Ruggieri, G. X. Peng, and M. Chernodub, *Phys. Rev. D* **94**, 054011 (2016), arXiv:1606.03287 [hep-ph].
- [58] M. Ruggieri, M. N. Chernodub, and Z.-Y. Lu, *Phys. Rev. D* **102**, 014031 (2020), arXiv:2004.09393 [hep-ph].
- [59] Y. Nambu and G. Jona-Lasinio, *Phys. Rev.* **122**, 345 (1961).
- [60] Y. Nambu and G. Jona-Lasinio, *Phys. Rev.* **124**, 246 (1961).
- [61] K. Fukushima, *Phys. Rev. D* **77**, 114028 (2008).
- [62] P. Costa, C. de Sousa, M. Ruivo, and Y. Kalinovsky, *Physics Letters B* **647**, 431 (2007).
- [63] Y. Lu, Y.-L. Du, Z.-F. Cui, and H.-S. Zong, *The European Physical Journal C* **75**, 495 (2015).
- [64] Y.-L. Du, Y. Lu, S.-S. Xu, Z.-F. Cui, C. Shi, and H.-S. Zong, *International Journal of Modern Physics A* **30**, 1550199 (2015), <https://doi.org/10.1142/S0217751X15501997>.
- [65] Z.-F. Cui, F.-Y. Hou, Y.-M. Shi, Y.-L. Wang, and H.-S. Zong, *Annals of Physics* **358**, 172 (2015), school of Physics at Nanjing University.
- [66] Y.-l. Du, Z.-f. Cui, Y.-h. Xia, and H.-s. Zong, *Phys. Rev. D* **88**, 114019 (2013).
- [67] S. Shi, Y.-C. Yang, Y.-H. Xia, Z.-F. Cui, X.-J. Liu, and H.-S. Zong, *Phys. Rev. D* **91**, 036006 (2015).
- [68] D. P. Menezes, M. B. Pinto, S. S. Avancini, and C. Providência, *Phys. Rev. C* **80**, 065805 (2009).
- [69] S. Ghosh, S. Mandal, and S. Chakrabarty, *Phys. Rev. C* **75**, 015805 (2007).
- [70] G. S. Bali, F. Bruckmann, G. Endrődi, Z. Fodor, S. D. Katz, and A. Schäfer, *Phys. Rev. D* **86**, 071502 (2012).
- [71] A. Yamamoto, *Phys. Rev. Lett.* **107**, 031601 (2011), arXiv:1105.0385 [hep-lat].
- [72] V. V. Braguta, E. M. Ilgenfritz, A. Y. Kotov, B. Petersson, and S. A. Skinderev, *Phys. Rev. D* **93**, 034509 (2016), arXiv:1512.05873 [hep-lat].
- [73] V. V. Braguta, V. A. Goy, E. M. Ilgenfritz, A. Y. Kotov, A. V. Molochkov, M. Muller-Preussker, and B. Petersson, *JHEP* **06**, 094 (2015), arXiv:1503.06670 [hep-lat].
- [74] A. Alexandru, G. Basar, and P. Bedaque, *Phys. Rev. D* **93**, 014504 (2016), arXiv:1510.03258 [hep-lat].
- [75] L. Scorzato, *PoS LATTICE2015*, 016 (2016), arXiv:1512.08039 [hep-lat].
- [76] V. V. Braguta and A. Y. Kotov, *Phys. Rev. D* **93**, 105025 (2016), arXiv:1601.04957 [hep-th].
- [77] J. I. Kapusta and C. Gale, *Finite-Temperature Field Theory: Principles and Applications*, 2nd ed., Cambridge Monographs on Mathematical Physics (Cambridge University Press, 2006).
- [78] R. P. Feynman, *International Journal of Theoretical Physics* **21**, 467 (1982).
- [79] B. Bauer, S. Bravyi, M. Motta, and G. K.-L. Chan, *Chemical Reviews* **120**, 12685–12717 (2020).
- [80] B. M. Terhal and D. P. DiVincenzo, *Phys. Rev. A* **61**, 022301 (2000).
- [81] D. Poulin and P. Wocjan, *Phys. Rev. Lett.* **103**, 220502 (2009).
- [82] A. Riera, C. Gogolin, and J. Eisert, *Phys. Rev. Lett.* **108**, 080402 (2012).
- [83] K. Temme, T. J. Osborne, K. G. Vollbrecht, D. Poulin, and F. Verstraete, *Nature* **471**, 87 (2011).
- [84] M.-H. Yung and A. Aspuru-Guzik, *Proceedings of the National Academy of Sciences* **109**, 754 (2012).
- [85] T. Li, X. Guo, W. K. Lai, X. Liu, E. Wang, H. Xing, D.-B. Zhang, and S.-L. Zhu, (2021), arXiv:2106.03865 [hep-ph].
- [86] D.-B. Zhang, H. Xing, H. Yan, E. Wang, and S.-L. Zhu, *Chin. Phys. B* **30**, 020306 (2021), arXiv:2011.01431 [quant-ph].
- [87] A. Tomiya, (2022), arXiv:2205.08860 [hep-lat].
- [88] X.-D. Xie, X. Guo, H. Xing, Z.-Y. Xue, D.-B. Zhang, and S.-L. Zhu (QuNu), *Phys. Rev. D* **106**, 054509 (2022), arXiv:2205.12767 [quant-ph].

- [89] Z. Davoudi, N. Mueller, and C. Powers, (2022), arXiv:2208.13112 [hep-lat].
- [90] F. Arute *et al.*, *Science* **369**, 1084 (2020), arXiv:2004.04174 [quant-ph].
- [91] H. Ma, M. Govoni, and G. Galli, *npj Computational Materials* **6**, 85 (2020).
- [92] A. Kandala, K. Temme, A. D. Córcoles, A. Mezzacapo, J. M. Chow, and J. M. Gambetta, *Nature* **567**, 491 (2019).
- [93] P. J. J. O’Malley, R. Babbush, I. D. Kivlichan, J. Romero, J. R. McClean, R. Barends, J. Kelly, P. Roushan, A. Tranter, N. Ding, B. Campbell, Y. Chen, Z. Chen, B. Chiaro, A. Dunsworth, A. G. Fowler, E. Jeffrey, E. Lucero, A. Megrant, J. Y. Mutus, M. Neeley, C. Neill, C. Quintana, D. Sank, A. Vainsencher, J. Wenner, T. C. White, P. V. Coveney, P. J. Love, H. Neven, A. Aspuru-Guzik, and J. M. Martinis, *Phys. Rev. X* **6**, 031007 (2016).
- [94] A. Kandala, A. Mezzacapo, K. Temme, M. Takita, M. Brink, J. M. Chow, and J. M. Gambetta, *Nature* **549**, 242 (2017).
- [95] A. Peruzzo, J. McClean, P. Shadbolt, M.-H. Yung, X.-Q. Zhou, P. J. Love, A. Aspuru-Guzik, and J. L. O’Brien, *Nature Communications* **5**, 4213 (2014).
- [96] J. I. Colless, V. V. Ramasesh, D. Dahmen, M. S. Blok, M. E. Kimchi-Schwartz, J. R. McClean, J. Carter, W. A. de Jong, and I. Siddiqi, *Phys. Rev. X* **8**, 011021 (2018).
- [97] A. Chiesa, F. Tacchino, M. Grossi, P. Santini, I. Tavernelli, D. Gerace, and S. Carretta, *Nature Physics* **15**, 455 (2019).
- [98] A. Smith, M. S. Kim, F. Pollmann, and J. Knolle, *npj Quantum Information* **5**, 106 (2019).
- [99] J. Zhang, G. Pagano, P. W. Hess, A. Kyprianidis, P. Becker, H. Kaplan, A. V. Gorshkov, Z. X. Gong, and C. Monroe, *Nature* **551**, 601 (2017).
- [100] R. Islam, C. Senko, W. C. Campbell, S. Korenblit, J. Smith, A. Lee, E. E. Edwards, C.-C. J. Wang, J. K. Freericks, and C. Monroe, *Science* **340**, 583 (2013).
- [101] A. Francis, J. K. Freericks, and A. F. Kemper, *Phys. Rev. B* **101**, 014411 (2020).
- [102] S. Lloyd, *Science* **273**, 1073 (1996).
- [103] W. A. De Jong, M. Metcalf, J. Mulligan, M. Płoskoń, F. Ringer, and X. Yao, *Phys. Rev. D* **104**, 051501 (2021), arXiv:2010.03571 [hep-ph].
- [104] W. A. de Jong, K. Lee, J. Mulligan, M. Płoskoń, F. Ringer, and X. Yao, (2021), arXiv:2106.08394 [quant-ph].
- [105] A. Wallraff, D. I. Schuster, A. Blais, L. Frunzio, R.-S. Huang, J. Majer, S. Kumar, S. M. Girvin, and R. J. Schoelkopf, *Nature* **431**, 162 (2004), bandiera_abtest: a Cg-type: Nature Research Journals Number: 7005 Primary_atype: Research Publisher: Nature Publishing Group.
- [106] J. Majer, J. M. Chow, J. M. Gambetta, J. Koch, B. R. Johnson, J. A. Schreier, L. Frunzio, D. I. Schuster, A. A. Houck, A. Wallraff, A. Blais, M. H. Devoret, S. M. Girvin, and R. J. Schoelkopf, *Nature* **449**, 443 (2007), bandiera_abtest: a Cg-type: Nature Research Journals Number: 7161 Primary_atype: Research Publisher: Nature Publishing Group.
- [107] S. P. Jordan, K. S. M. Lee, and J. Preskill, *Science* **336**, 1130 (2012), arXiv: 1111.3633.
- [108] E. Zohar, J. I. Cirac, and B. Reznik, *Physical Review Letters* **109**, 125302 (2012), publisher: American Physical Society.
- [109] E. Zohar, J. I. Cirac, and B. Reznik, *Physical Review Letters* **110**, 125304 (2013), publisher: American Physical Society.
- [110] D. Banerjee, M. Bögli, M. Dalmonte, E. Rico, P. Stebler, U.-J. Wiese, and P. Zoller, *Physical Review Letters* **110**, 125303 (2013), publisher: American Physical Society.
- [111] D. Banerjee, M. Dalmonte, M. Müller, E. Rico, P. Stebler, U.-J. Wiese, and P. Zoller, *Physical Review Letters* **109**, 175302 (2012), arXiv: 1205.6366.
- [112] U.-J. Wiese, *Annalen der Physik* **525**, 777 (2013), eprint: https://onlinelibrary.wiley.com/doi/pdf/10.1002/andp.201300104.
- [113] U.-J. Wiese, *Nuclear Physics A QUARK MATTER 2014*, **931**, 246 (2014).
- [114] S. P. Jordan, K. S. M. Lee, and J. Preskill, arXiv:1404.7115 [hep-th, physics:quant-ph] (2014), arXiv: 1404.7115.
- [115] L. García-Álvarez, J. Casanova, A. Mezzacapo, I. L. Egusquiza, L. Lamata, G. Romero, and E. Solano, *Physical Review Letters* **114**, 070502 (2015), publisher: American Physical Society.
- [116] D. Marcos, P. Widmer, E. Rico, M. Hafezi, P. Rabl, U. J. Wiese, and P. Zoller, *Annals of Physics* **351**, 634 (2014).
- [117] A. Bazavov, Y. Meurice, S.-W. Tsai, J. Unmuth-Yockey, and J. Zhang, *Physical Review D* **92**, 076003 (2015), publisher: American Physical Society.
- [118] E. Zohar, J. I. Cirac, and B. Reznik, *Reports on Progress in Physics* **79**, 014401 (2015), publisher: IOP Publishing.
- [119] A. Mezzacapo, E. Rico, C. Sabín, I. L. Egusquiza, L. Lamata, and E. Solano, *Physical Review Letters* **115**, 240502 (2015), publisher: American Physical Society.
- [120] M. Dalmonte and S. Montangero, *Contemporary Physics* **57**, 388 (2016), arXiv: 1602.03776.
- [121] E. Zohar, A. Farace, B. Reznik, and J. I. Cirac, *Physical Review A* **95**, 023604 (2017), arXiv: 1607.08121.
- [122] E. A. Martinez, C. A. Muschik, P. Schindler, D. Nigg, A. Erhard, M. Heyl, P. Hauke, M. Dalmonte, T. Monz, P. Zoller, and R. Blatt, *Nature* **534**, 516 (2016), arXiv: 1605.04570.
- [123] A. Bermudez, G. Aarts, and M. Müller, *Physical Review X* **7**, 041012 (2017), publisher: American Physical Society.
- [124] J. M. Gambetta, J. M. Chow, and M. Steffen, *npj Quantum Information* **3**, 1 (2017), bandiera_abtest: a Cc_license_type: cc_by Cg_type: Nature Research Journals Number: 1 Primary_atype: Reviews Publisher: Nature Publishing Group Subject_term: Quantum information;Qubits Subject_term_id: quantum-information;qubits.
- [125] L. Krinner, M. Stewart, A. Pazmiño, J. Kwon, and D. Schneble, *Nature* **559**, 589 (2018), bandiera_abtest: a Cg-type: Nature Research Journals Number: 7715 Primary_atype: Research Publisher: Nature Publishing Group Subject_term: Matter waves and particle beams;Quantum simulation;Single photons and quantum effects;Ultracold gases Subject_term_id: matter-waves-and-particle-beams;quantum-simulation;single-photons-and-quantum-effects;ultracold-gases.

- [126] A. Macridin, P. Spentzouris, J. Amundson, and R. Harnik, *Physical Review Letters* **121**, 110504 (2018), publisher: American Physical Society.
- [127] T. V. Zache, F. Hebenstreit, F. Jendrzejewski, M. K. Oberthaler, J. Berges, and P. Hauke, *Quantum Science and Technology* **3**, 034010 (2018), publisher: IOP Publishing.
- [128] J. Zhang, J. Unmuth-Yockey, J. Zeiher, A. Bazavov, S.-W. Tsai, and Y. Meurice, *Physical Review Letters* **121**, 223201 (2018), publisher: American Physical Society.
- [129] N. Klco, E. F. Dumitrescu, A. J. McCaskey, T. D. Morris, R. C. Pooser, M. Sanz, E. Solano, P. Lougovski, and M. J. Savage, *Physical Review A* **98**, 032331 (2018), arXiv: 1803.03326.
- [130] N. Klco and M. J. Savage, *Physical Review A* **99**, 052335 (2019), arXiv: 1808.10378.
- [131] E. Gustafson, Y. Meurice, and J. Unmuth-Yockey, *Physical Review D* **99**, 094503 (2019), publisher: American Physical Society.
- [132] NuQS Collaboration, A. Alexandru, P. F. Bedaque, H. Lamm, and S. Lawrence, *Physical Review Letters* **123**, 090501 (2019), publisher: American Physical Society.
- [133] G. Magnifico, M. Dalmonte, P. Facchi, S. Pascazio, F. V. Pepe, and E. Ercolessi, *Quantum* **4**, 281 (2020), arXiv: 1909.04821.
- [134] S. P. Jordan, K. S. M. Lee, and J. Preskill, arXiv:1112.4833 [hep-th, physics:quant-ph] (2019), arXiv: 1112.4833.
- [135] H.-H. Lu, N. Klco, J. M. Lukens, T. D. Morris, A. Bansal, A. Ekström, G. Hagen, T. Papenbrock, A. M. Weiner, M. J. Savage, and P. Lougovski, *Physical Review A* **100**, 012320 (2019), arXiv: 1810.03959.
- [136] N. Klco and M. J. Savage, *Physical Review A* **102**, 012612 (2020), arXiv: 1904.10440.
- [137] H. Lamm and S. Lawrence, *Physical Review Letters* **121**, 170501 (2018), arXiv: 1806.06649.
- [138] N. Klco, J. R. Stryker, and M. J. Savage, *Physical Review D* **101**, 074512 (2020), arXiv: 1908.06935.
- [139] A. Alexandru, P. F. Bedaque, S. Harmalkar, H. Lamm, S. Lawrence, and N. C. Warrington, *Physical Review D* **100**, 114501 (2019), arXiv: 1906.11213.
- [140] N. Mueller, A. Tarasov, and R. Venugopalan, *Physical Review D* **102**, 016007 (2020), arXiv: 1908.07051.
- [141] H. Lamm, S. Lawrence, and Y. Yamauchi, *Physical Review Research* **2**, 013272 (2020), arXiv: 1908.10439.
- [142] B. Chakraborty, M. Honda, T. Izubuchi, Y. Kikuchi, and A. Tomiya, arXiv:2001.00485 [cond-mat, physics:hep-lat, physics:hep-ph, physics:hep-th, physics:quant-ph] (2020), arXiv: 2001.00485.
- [143] A. Bermudez, E. Tirrito, M. Rizzi, M. Lewenstein, and S. Hands, *Annals Phys.* **399**, 149 (2018), arXiv:1807.03202 [cond-mat.quant-gas].
- [144] L. Ziegler, E. Tirrito, M. Lewenstein, S. Hands, and A. Bermudez, (2020), arXiv:2011.08744 [cond-mat.quant-gas].
- [145] L. Ziegler, E. Tirrito, M. Lewenstein, S. Hands, and A. Bermudez, (2021), arXiv:2111.04485 [cond-mat.quant-gas].
- [146] S.-N. Sun, M. Motta, R. N. Tazhigulov, A. T. Tan, G. K.-L. Chan, and A. J. Minnich, *PRX Quantum* **2**, 010317 (2021).
- [147] J.-L. Ville *et al.*, (2021), arXiv:2104.08785 [quant-ph].
- [148] A. M. Czajka, Z.-B. Kang, H. Ma, and F. Zhao, *JHEP* **08**, 209 (2022), arXiv:2112.03944 [hep-ph].
- [149] D. J. Gross and A. Neveu, *Phys. Rev. D* **10**, 3235 (1974).
- [150] S. Borsanyi, G. Endrodi, Z. Fodor, A. Jakovac, S. D. Katz, S. Krieg, C. Ratti, and K. K. Szabo, *JHEP* **11**, 077 (2010), arXiv:1007.2580 [hep-lat].
- [151] J. Kogut and L. Susskind, *Phys. Rev. D* **11**, 395 (1975).
- [152] S. Borsanyi, Z. Fodor, C. Hoelbling, S. D. Katz, S. Krieg, and K. K. Szabo, *Phys. Lett. B* **730**, 99 (2014), arXiv:1309.5258 [hep-lat].
- [153] Y. Aoki, Z. Fodor, S. D. Katz, and K. K. Szabo, *JHEP* **01**, 089 (2006), arXiv:hep-lat/0510084.
- [154] A. Bazavov *et al.* (HotQCD), *Phys. Rev. D* **90**, 094503 (2014), arXiv:1407.6387 [hep-lat].
- [155] C. Aubin, T. Blum, C. Tu, M. Golterman, C. Jung, and S. Peris, *Phys. Rev. D* **101**, 014503 (2020), arXiv:1905.09307 [hep-lat].
- [156] P. Jordan and E. Wigner, *Zeitschrift für Physik* **47**, 631 (1928).
- [157] H. F. Trotter, *Proceedings of the American Mathematical Society* **10**, 545 (1959).
- [158] M. Suzuki, *Communications in Mathematical Physics* **51**, 183 (1976).
- [159] M. Motta, C. Sun, A. T. K. Tan, M. J. O'Rourke, E. Ye, A. J. Minnich, F. G. S. L. Brandão, and G. K.-L. Chan, *Nature Physics* **16**, 205 (2020).
- [160] B. M. Terhal and D. P. DiVincenzo, *Phys. Rev. A* **61**, 22301 (2000), arXiv:quant-ph/9810063.
- [161] K. Temme, T. J. Osborne, K. G. Vollbrecht, D. Poulin, and F. Verstraete, *Nature* **471**, 87 (2011), arXiv:0911.3635 [quant-ph].
- [162] A. N. Chowdhury and R. D. Somma, (2016), 10.48550/ARXIV.1603.02940.
- [163] F. G. S. L. Brandão and M. J. Kastoryano, *Commun. Math. Phys.* **365**, 1 (2019), arXiv:1609.07877 [quant-ph].
- [164] S. Barison, F. Vicentini, I. Cirac, and G. Carleo, (2022), arXiv:2204.03454 [quant-ph].
- [165] P. D. Johnson, A. A. Kunitsa, J. F. Gonthier, M. D. Radin, C. Buda, E. J. Doskocil, C. M. Abuan, and J. Romero, (2022), arXiv:2203.07275 [quant-ph].
- [166] C. Cao, Y. Yu, Z. Wu, N. Shannon, B. Zeng, and R. Joynt, (2021), arXiv:2109.08132 [quant-ph].
- [167] K. Omiya*, Y. O. Nakagawa*, S. Koh, W. Mizukami, Q. Gao, and T. Kobayashi, *J. Chem. Theor. Comput.* **18**, 741 (2022), arXiv:2107.12705 [physics.chem-ph].
- [168] N. H. Stair and F. A. Evangelista, “Qforte: an efficient state simulator and quantum algorithms library for molecular electronic structure,” (2021), arXiv:2108.04413 [quant-ph].
- [169] M. S. ANIS, Abby-Mitchell, H. Abraham, AduOffei, R. Agarwal, G. Agliardi, M. Aharoni, I. Y. Akhalwaya, G. Aleksandrowicz, T. Alexander, M. Amy, S. Anagolum, Anthony-Gandon, E. Arbel, A. Asfaw, A. Athalye, A. Avkhadiev, C. Azaustre, P. Bhole, A. Banerjee, S. Banerjee, W. Bang, A. Bansal, P. Barkoutsos, A. Barnawal, G. Barron, G. S. Barron, L. Bello, Y. Ben-Haim, M. C. Bennett, D. Bevenius, D. Bhatnagar, A. Bhobe, P. Bianchini, L. S. Bishop, C. Blank, S. Bolos, S. Bopardikar, S. Bosch, S. Brandhofer, Brandon, S. Bravyi, N. Bronn, Bryce-Fuller, D. Bucher, A. Burov, F. Cabrera, P. Calpin, L. Capelluto, J. Carballo, G. Carrascal, A. Carriker, I. Carvalho, A. Chen, C.-F. Chen, E. Chen, J. C.

- Chen, R. Chen, F. Chevallier, K. Chinda, R. Cholaramjan, J. M. Chow, S. Churchill, CisterMoke, C. Claus, C. Clauss, C. Clothier, R. Cocking, R. Cocuzzo, J. Connor, F. Correa, Z. Crockett, A. J. Cross, A. W. Cross, S. Cross, J. Cruz-Benito, C. Culver, A. D. Córcoles-Gonzales, N. D. S. Dague, T. E. Dandachi, A. N. Dangwal, J. Daniel, M. Daniels, M. Dartailh, A. R. Davila, F. Debouni, A. Dekusar, A. Deshmukh, M. Deshpande, D. Ding, J. Doi, E. M. Dow, E. Drechsler, E. Dumitrescu, K. Dumon, I. Duran, K. EL-Safty, E. Eastman, G. Eberle, A. Ebrahimi, P. Eendebak, D. Egger, ElePT, Emilio, A. Espiricueta, M. Everitt, D. Facoetti, Farida, P. M. Fernández, S. Ferracin, D. Ferrari, A. H. Ferrera, R. Foulland, A. Frisch, A. Fuhrer, B. Fuller, M. GEORGE, J. Gacon, B. G. Gago, C. Gambella, J. M. Gambetta, A. Gammapila, L. Garcia, T. Garg, S. Garion, J. R. Garrison, T. Gates, L. Gil, A. Gilliam, A. Giridharan, J. Gomez-Mosquera, Gonzalo, S. de la Puente González, J. Gorzinski, I. Gould, D. Greenberg, D. Grinko, W. Guan, D. Guijo, J. A. Gunnels, H. Gupta, N. Gupta, J. M. Günther, M. Haglund, I. Haide, I. Hamamura, O. C. Hamido, F. Harkins, K. Hartman, A. Hasan, V. Havlicek, J. Hellmers, L. Herok, S. Hillmich, H. Horii, C. Howington, S. Hu, W. Hu, J. Huang, R. Huisman, H. Imai, T. Imamichi, K. Ishizaki, Ishwor, R. Iten, T. Itoko, A. Ivrii, A. Javadi, A. Javadi-Abhari, W. Javed, Q. Jianhua, M. Jivrajani, K. Johns, S. Johnstun, Jonathan-Shoemaker, JosDenmark, Josh-Dumo, J. Judge, T. Kachmann, A. Kale, N. Kanazawa, J. Kane, Kang-Bae, A. Kapila, A. Karazeev, P. Kassebaum, J. Kelso, S. Kelso, V. Khanderao, S. King, Y. Kobayashi, Kovi11Day, A. Kovyrshin, R. Krishnamuram, V. Krishnan, K. Krsulich, P. Kumkar, G. Kus, R. LaRose, E. Lacal, R. Lambert, H. Landa, J. Lapeyre, J. Latone, S. Lawrence, C. Lee, G. Li, J. Lishman, D. Liu, P. Liu, Lolcroc, A. K. M, L. Madden, Y. Maeng, S. Maheshkar, K. Majmudar, A. Malyshov, M. E. Mandouh, J. Manela, Manjula, J. Marecek, M. Marques, K. Marwaha, D. Maslov, P. Maszota, D. Mathews, A. Matsuo, F. Mazhandu, D. McClure, M. McElaney, C. McGarry, D. McKay, D. McPhereson, S. Meesala, D. Meirom, C. Mendell, T. Metcalfe, M. Mevissen, A. Meyer, A. Mezzacapo, R. Midha, D. Miller, Z. Minev, A. Mitchell, N. Moll, A. Montanez, G. Monteiro, M. D. Mooring, R. Morales, N. Moran, D. Morcuende, S. Mostafa, M. Motta, R. Moyard, P. Murali, J. Müggenburg, T. NEMOZ, D. Nadlinger, K. Nakanishi, G. Nannicini, P. Nation, E. Navarro, Y. Naveh, S. W. Neagle, P. Neuweiler, A. Ngoueya, J. Nicander, Nick-Singstock, P. Niroula, H. Norlen, NuoWenLei, L. J. O’Riordan, O. Ogunbayo, P. Ollitrault, T. Onodera, R. Otaolea, S. Oud, D. Padilha, H. Paik, S. Pal, Y. Pang, A. Panigrahi, V. R. Pascuzzi, S. Perriello, E. Peterson, A. Phan, K. Pilch, F. Piro, M. Pistoia, C. Piveteau, J. Plewa, P. Pooreau, A. Pozas-Kerstjens, R. Pracht, M. Prokop, V. Prutyanov, S. Puri, D. Puzzuoli, J. Pérez, Quant02, Quintiii, R. I. Rahaman, A. Raja, R. Rajeev, I. Rajput, N. Ramagiri, A. Rao, R. Raymond, O. Reardon-Smith, R. M.-C. Redondo, M. Reuter, J. Rice, M. Riedemann, Rietesh, D. Risinger, M. L. Rocca, D. M. Rodríguez, RohithKarur, B. Rosand, M. Rossmannek, M. Ryu, T. SAPV, N. R. C. Sa, A. Saha, A. Ash-Saki, S. Sanand, M. Sandberg, H. Sandesara, R. Sapra, H. Sargsyan, A. Sarkar, N. Sathaye, B. Schmitt, C. Schnabel, Z. Schoenfeld, T. L. Scholten, E. Schoute, M. Schutterbrandt, J. Schwarm, J. Seaward, Sergi, I. F. Sertage, K. Setia, F. Shah, N. Shammah, R. Sharma, Y. Shi, J. Shoemaker, A. Silva, A. Simonetto, D. Singh, D. Singh, P. Singh, P. Singkanipa, Y. Siraichi, Siri, J. Sistos, I. Siddikov, S. Sivarajah, M. B. Sletfjerdning, J. A. Smolin, M. Soeken, I. O. Sokolov, I. Sokolov, V. P. Soloviev, SooluThomas, Starfish, D. Steenken, M. Styppulkoski, A. Suau, S. Sun, K. J. Sung, M. Suwama, O. Słowiak, H. Takahashi, T. Takawale, I. Tavernelli, C. Taylor, P. Taylour, S. Thomas, K. Tian, M. Tillet, M. Tod, M. Tomasik, C. Tornow, E. de la Torre, J. L. S. Toural, K. Trabing, M. Treinish, D. Trenev, TrishaPe, F. Truger, G. Tsilimigkounakis, D. Tulsi, W. Turner, Y. Vaknin, C. R. Valcarce, F. Varchon, A. Vartak, A. C. Vazquez, P. Vijaywargiya, V. Villar, B. Vishnu, D. Vogt-Lee, C. Vuillot, J. Weaver, J. Weidenfeller, R. Wieczorek, J. A. Wildstrom, J. Wilson, E. Winston, WinterSoldier, J. J. Woehr, S. Werner, R. Woo, C. J. Wood, R. Wood, S. Wood, J. Wootton, M. Wright, L. Xing, J. YU, B. Yang, U. Yang, J. Yao, D. Yerulin, R. Yonekura, D. Yonge-Mallo, R. Yoshida, R. Young, J. Yu, L. Yu, C. Zuchow, L. Zdanski, H. Zhang, I. Zidaru, C. Zoufal, aeddins ibm, alexzhang13, b63, bartek bartlomiej, bcamorrison, brandhsn, charmerDark, deeplokhande, dekel.meirom, dime10, dlasecki, ehchen, fanizzamarco, fs1132429, gadijal, galeinston, georgezhou20, georgios ts, gruu, hhori, hykavitha, itoko, jeppevinkel, jessica angel7, jezerjojo14, jliu45, jscott2, klinvill, krutik2966, ma5x, michelle4654, msuwama, nico lgrs, ntgiwsvp, ord-moj, sagar pahwa, pritamsinha2304, ryancocuzzo, saktar unr, saswati qiskit, septembr, sethmerkel, sg495, shaashwat, smturro2, sternparky, strickroman, tiger-jack, tsura crisaldo, vadebayo49, welien, willhbang, wmurphy collabstar, yang.luh, and M. Čepulkovskis, “Qiskit: An open-source framework for quantum computing,” (2021).
- [170] “Ibm quantum,” .
- [171] D. J. Gross, R. D. Pisarski, and L. G. Yaffe, *Rev. Mod. Phys.* **53**, 43 (1981).
- [172] Y. Nambu and G. Jona-Lasinio, *Phys. Rev.* **122**, 345 (1961).
- [173] L. D. McLerran and B. Svetitsky, *Phys. Rev. D* **24**, 450 (1981).
- [174] A. Polyakov, *Physics Letters B* **72**, 477 (1978).
- [175] Z. Fang, Y.-L. Wu, and L. Zhang, *Phys. Rev. D* **98**, 114003 (2018), arXiv:1805.05019 [hep-ph].
- [176] J. Walecka, *Annals of Physics* **83**, 491 (1974).
- [177] H. Ohata and H. Suganuma, *Phys. Rev. D* **103**, 054505 (2021), arXiv:2012.03537 [hep-lat].
- [178] N. Carabba and E. Meggiolaro, *Phys. Rev. D* **105**, 054034 (2022), arXiv:2106.10074 [hep-ph].
- [179] R. S. Smith, M. J. Curtis, and W. J. Zeng, “A practical quantum instruction set architecture,” (2016).
- [180] J. S. Kottmann, S. Alperin-Lea, T. Tamayo-Mendoza, A. Cervera-Lierta, C. Lavigne, T.-C. Yen, V. Verteletskyi, P. Schleich, A. Anand, M. Degroote, S. Chaney, M. Kesibi, N. G. Curnow, B. Solo, G. Tsilimigkounakis, C. Zendejas-Morales, A. F. Izmaylov, and A. Aspuru-Guzik, *Quantum Science and Technology* **6**, 024009 (2021).

- [181] “Q# language and core libraries design,” <Https://github.com/microsoft/qsharp-language>.
- [182] G. Aleksandrowicz, T. Alexander, P. Barkoutsos, L. Bello, Y. Ben-Haim, D. Bucher, F. J. Cabrera-Hernández, J. Carballo-Franquis, A. Chen, C.-F. Chen, J. M. Chow, A. D. Córcoles-Gonzales, A. J. Cross, A. Cross, J. Cruz-Benito, C. Culver, S. D. L. P. González, E. D. L. Torre, D. Ding, E. Dumitrescu, I. Duran, P. Eendebak, M. Everitt, I. F. Sertage, A. Frisch, A. Fuhrer, J. Gambetta, B. G. Gago, J. Gomez-Mosquera, D. Greenberg, I. Hamamura, V. Havlicek, J. Hellmers, Łukasz Herok, H. Horii, S. Hu, T. Imamichi, T. Itoko, A. Javadi-Abhari, N. Kanazawa, A. Karazeev, K. Krsulich, P. Liu, Y. Luh, Y. Maeng, M. Marques, F. J. Martín-Fernández, D. T. McClure, D. McKay, S. Meesala, A. Mezzacapo, N. Moll, D. M. Rodríguez, G. Nannicini, P. Nation, P. Ollitrault, L. J. O’Riordan, H. Paik, J. Pérez, A. Phan, M. Pistoia, V. Prutyanov, M. Reuter, J. Rice, A. R. Davila, R. H. P. Rudy, M. Ryu, N. Sathaye, C. Schnabel, E. Schoute, K. Setia, Y. Shi, A. Silva, Y. Siraichi, S. Sivarajah, J. A. Smolin, M. Soeken, H. Takahashi, I. Tavernelli, C. Taylor, P. Taylour, K. Trabing, M. Treinish, W. Turner, D. Vogt-Lee, C. Vuillot, J. A. Wildstrom, J. Wilson, E. Winston, C. Wood, S. Wood, S. Wörner, I. Y. Akhalwaya, and C. Zoufal, [\(2019\), 10.5281/zenodo.2562111](https://doi.org/10.5281/zenodo.2562111).
- [183] A. J. McCaskey, D. I. Lyakh, E. F. Dumitrescu, S. S. Powers, and T. S. Humble, *Quantum Science and Technology* **5**, 024002 (2020).
- [184] N. C. Rubin, K. Gunst, A. White, L. Freitag, K. Throssell, G. K.-L. Chan, R. Babbush, and T. Shiozaki, *Quantum* **5**, 568 (2021), [arXiv:2104.13944 \[quant-ph\]](https://arxiv.org/abs/2104.13944).
- [185] C. Developers, “Cirq,” (2021), See full list of authors on Github: <https://github.com/quantumlib/Cirq/graphs/contributors>.
- [186] K. Bharti *et al.*, *Rev. Mod. Phys.* **94**, 015004 (2022), [arXiv:2101.08448 \[quant-ph\]](https://arxiv.org/abs/2101.08448).
- [187] A. Anand, P. Schleich, S. Alperin-Lea, P. W. K. Jensen, S. Sim, M. Díaz-Tinoco, J. S. Kottmann, M. Degroote, A. F. Izmaylov, and A. Aspuru-Guzik, <https://doi.org/10.1039/D1CS00932J>, [arXiv:2109.15176 \[quant-ph\]](https://arxiv.org/abs/2109.15176).